NHC

Property of
NOAA Coral Gables Library
Gables One Tower
1320 South Dixie Highway, Room 520
Coral Gables, Florida 33145

QC
995
.U672
no.44

NOAA Technical Memorandum NWS NHC-44

A REVISED NATIONAL HURRICANE CENTER

NHC83 MODEL (NHC90)

Prepared by:

Charles J. Neumann
Science Applications International Corporation

Contract No. 50DSNC-8-00141

and

Colin J. McAdie
National Hurricane Center

National Hurricane Center
Coral Gables, Florida
November 1991

839

TED STATES
PARTMENT OF COMMERCE
ert A. Mosbacher, Secretary

National Oceanic and Atmospheric Administration
John A. Knauss
Under Secretary and Administrator

National Weather Service
Elbert W. Friday
Assistant Administrator

TABLE OF CONTENTS

Abstract. 1

1. Background. 1
1.1 Tropical cyclone prediction models 1
1.1.1 Introduction. 1
1.1.2 Types of motion models. 1
1.1.3 Statistical-dynamical models. 2
1.2 The NHC83 model. 2
1.2.1 Performance of NHC83. 2
1.2.2 Can NHC83 be improved?. 4
1.3 Purpose of study 4

2. Model deficiencies. 4
2.1 Non-correctable (external) deficiencies. 5
2.1.1 Reliance on numerical guidance. 5
2.1.2 Initial motion vectors. 7
2.2 Partially correctable (external) deficiencies. 7
2.2.1 Initial analyses problems 7
2.2.2 Bias in numerical forecasts 9
2.3 Correctable deficiencies 10
2.3.1 Inconsistencies in NHC83 forecast track 10
2.3.2 Inconsistencies in NHC83 stratification scheme. . .10
2.3.3 Geographical limitations in development data. . . .11
2.3.4 Predictor selection logic 11
2.3.5 Graphical output. 12
2.4 Summary of differences between NHC83 and NHC90 12

3. Development of the NHC90 model. 12
3.1 Introduction 12
3.2 Developmental data 13
3.2.1 Sample size 13
3.2.2 Stratification. 13
3.2.3 Statistical attributes of development data. 14
3.2.4 Composite analyses. 15
3.3 Selection of predictors. 17
3.3.1 Analysis mode vs. perfect-prog mode 17
3.3.2 Selection criteria. 17
3.3.3 Pairing of predictors 18
3.3.4 Example of predictor selection, North Zone, along track 18
3.3.5 Examples of predictor selection, North Zone, across track 20
3.3.6 Example of predictor selection, South Zone, along track 20
3.3.7 Final selection of predictors 20

4. Model performance on development data 23
4.1 Reductions of variance 23
4.1.1 Review of model structure 23
4.1.2 Comparison of variance reductions 23
4.2 Forecast error 27

5. Graphics package. 29
5.1 NHC83 graphics package 29
5.2 NHC90 graphics package 29

6. Potential for additional improvement to NHC90 30
6.1 Grid rotation. 30
6.1.1 The NHC83/NHC90 system. 30
6.1.2 Proposed NHC90 grid rotation system 30
6.2 Use of winds rather than heights 33

7. References. 34

A REVISED NATIONAL HURRICANE CENTER NHC83 MODEL (NHC90)

Charles J. Neumann
Science Applications International Corporation[1]

Colin J. McAdie
National Hurricane Center

ABSTRACT

The National Hurricane Center (NHC) statistical-dynamical NHC83 model was introduced operationally for the 1983 hurricane season. Based on a number of evaluation criteria such as timeliness, availability, overall utility and minimum error, NHC83, through the 1988 hurricane season, has outperformed other models in use at NHC by a rather wide margin. Accordingly, this type of prediction model appears to be very sound. Nevertheless, long-term operational use of the model has disclosed certain design weaknesses. These are reviewed. The question is posed as to the potential for still further improvement to NHC83 by addressing and correcting these deficiencies.

Two approaches to potential improvement are suggested. The first involves maintaining the basic integrity of the model but using deep-layer-mean winds rather than deep-layer-mean geopotential heights as the main source of predictive information. The second method involves retaining the geopotential heights as predictors but revising the model based upon an evaluation of NHC83 1983-1988 error patterns.

Each method appeared to have considerable merit and both were undertaken. This study reports on a revision to the model using the second of the two approaches; that is, maintaining the height fields but addressing identifiable deficiencies. Forecast errors obtained from developmental data, when compared to those of the original NHC83 model, suggest that the new model (NHC90) should outperform NHC83. However, this must still be confirmed through one or more years of operational testing.

The other approach, that is, revising the model using deep-layer-mean winds rather than heights, is still under development and is discussed briefly in Section 6.

1. BACKGROUND

1.1 TROPICAL CYCLONE PREDICTION MODELS

1.1.1 Introduction - Preparatory to the issuance of tropical cyclone advisories, the National Hurricane Center (NHC) activates a number of models which provide objective guidance on various aspects of tropical cyclone prediction. Essentially, these models fall into three categories: those for the prediction of (1) tropical cyclone motion, (2) tropical cyclone intensity and (3) storm surge. Efforts are continually underway at NHC and elsewhere to improve on the performance of these models. This study reports on recent and proposed improvements to the NHC83 model, one of the principal NHC models for guidance on tropical cyclone motion.

1.1.2 Types of Motion Models - In the broadest sense, models for the prediction of tropical cyclone motion can be classified as being either statistical or dynamical (numerical). Depending on the method of treating developmental data and the type of predictors employed,

---

[1] Prepared for the National Hurricane Center, Coral Gables, FL 33146: Contract Number 50DSNC-8-00141. Contract partially supported by NOAA/ERL AOML-Hurricane Research Division (HRD).

the statistical models are sub-classified as being analog, CLIPER-class or statistical-synoptic. The dynamical (numerical) models, depending on sophistication, assumptions and other factors, are designated as being either barotropic or baroclinic. Models which use output from a dynamical (numerical) model but treat these data in a statistical prediction framework, are referred to as statistical- dynamical.

Statistical and dynamical models have many unique advantages, disadvantages and other attributes such that both types are complimentary and most tropical cyclone forecast centers maintain one or more models in each category. Further discussion of the models in use at the NHC is provided by Neumann and Pelissier (1981a, 1981b) while a more general discussion is provided by McBride and Holland (1987) and Elsberry et al. (1987).

1.1.3 Statistical-dynamical Models - Conceptually, statistical-dynamical models are very appealing in that they combine the advantages of both the statistical and dynamical approach to tropical cyclone prediction. However, structuring such models to function properly in an operational environment presents many problems. Foremost among these is the requirement that developmental and operational data maintain similar statistical characteristics. Because of frequent changes in operational procedures, this is difficult to comply with. Indeed, the statistical-dynamical NHC73 model (Neumann and Lawrence, 1975), which performed very well following its introduction in 1973, was recently discontinued at the NHC because of this statistical pitfall. The model was insufficiently robust to withstand changes in the numerical model package which provided input.

1.2 THE NHC83 MODEL

1.2.1 Performance of NHC83 - The statistical-dynamical NHC83 model (Neumann, 1988)[2] was introduced at NHC for the 1983 hurricane season. With lessons learned from the NHC73 model, NHC83 was designed with sufficient robustness to withstand reasonable changes in the statistical characteristics of the large-scale numerical model[3] which feeds into NHC83. Nevertheless, changes to the large-scale model have caused and will continue to cause at least some problems with NHC83; these will be discussed in a later section.

Based on various performance "yardsticks" such as reliability, availability and minimum forecast error, the NHC83 model, for a number of years, has routinely outperformed other operational models in use at the National Hurricane Center. Table 1, illustrates the magnitude of NHC83 errors over the six-year period 1983 through 1988. The excellent performance of the model, relative to other models, has been unusually consistent from one year to the next.

---

[2] For convenience, this document will hereinafter be referred to as TM41.

[3] Currently, forecasts generated by the National Meteorological Center Global Spectral Model, both the Medium Range Forecast (MRF), and aviation run are utilized by NHC83. Details are provided in TM41, Table 11.

AVERAGE FORECAST ERRORS (n mi) FOR EACH YEAR, 1983-1988

		NHC83	CLIPER	NHC72	OFFICIAL	NHC73	SAMPLE SIZE
	12H	26*	30	32	39	32	08
1983	24H	49*	63	67	81	90	05
	48H	166	140*	149	223	213	03
	72H	374*	441	666	397	417	02
	12H	48*	53	50	53	50	65
1984	24H	96*	119	104	116	119	57
	48H	217*	260	252	224	243	47
	72H	324*	332	422	341	419	37
	12H	48*	53	57	48*	50	75
1985	24H	88*	117	128	100	107	66
	48H	168*	271	290	222	242	44
	72H	288*	399	367	333	466	26
	12H	43	47	42*	44	43	35
1986	24H	88*	109	95	101	99	29
	48H	173*	241	210	230	228	17
	72H	294*	377	405	387	429	11
	12H	47	52	51	47	41*	33
1987	24H	103*	140	147	114	109	30
	48H	222*	391	365	233	293	24
	72H	313*	638	556	365	466	19
	12H	35*	38	---	36	---	66
1988	24H	58*	74	---	62	---	59
	48H	129*	175	---	138	---	50
	72H	193*	282	---	222	---	40
1983	12H	43.6*	48.1	50.6	45.5	46.8	282
THRU	24H	84.3*	108.9	117.0	97.0	109.3	246
1988#	48H	177.4*	252.9	276.9	201.9	249.0	185
	72H	274.4*	377.7	436.9	311.5	442.4	135
		NHC83	CLIPER	NHC72	OFFICIAL	NHC73	SAMPLE SIZE

Summary for NHC72 and NHC73 models does not include 1988 season.

Table 1. Average forecast errors (operational) of specified model for each year, 1983 - 1988, and over the entire 6-year period. Asterisk (*) designates minimum error for specified model for given forecast period. Sample is homogeneous and combines 0000 and 1200 UTC forecasts. The CLIPER, NHC72 (statistical-synoptic) and NHC73 (statistical-dynamical) are described by Neumann and Pelissier (1981a). NHC83 is described by Neumann (1988).

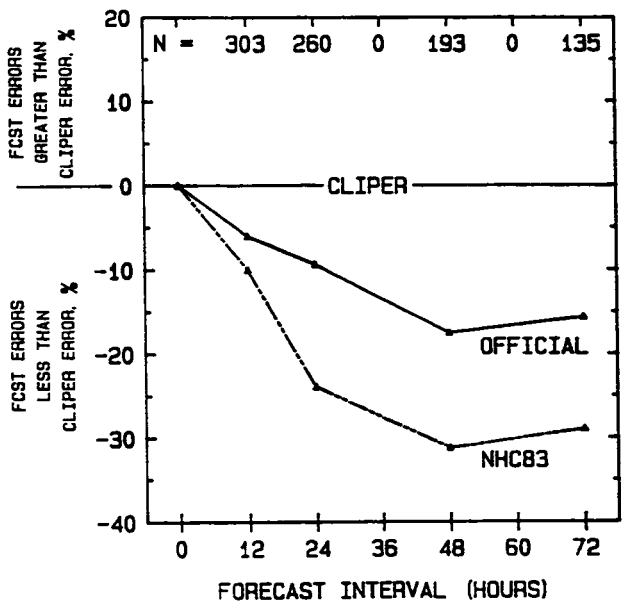

Fig. 1. Performance of NHC83 and "Official Forecasts" relative to CLIPER model. Sample is homogeneous and extends from 1983 through 1988. Number of cases (specified across upper portion of chart) is generally greater than that given in Table 1 due to exclusion of NHC72 and NHC73 models.

One of the advantages of NHC83 is the excellent performance at the important 24 h projection. This is demonstrated in Fig. 1 where a rapid improvement over climatology and persistence (CLIPER), 0 through 24 h (and beyond) is evident. This can be attributed to: (1) large scale "steering" information contained in the National Meteorological Center (NMC) Global Spectral Model used by NHC83, (2) NHC83 methodology used in extracting this information and (3) the NHC83 rotated grid system (Shapiro and Neumann, 1984).

1.2.2 Can NHC83 be improved? - The predictive skill of NHC83 is obtained from forecast deep-layer-mean geopotential height fields derived from various runs of the NMC global spectral model (see footnote 3).

Given the excellent performance of NHC83, further improvement might not seem necessary; however, close monitoring of forecasts from the model during the period, 1983-1988, disclosed several design weaknesses which were amenable to correction. Additionally, the current NHC83 model was developed from an analysis domain which did not extend into the deep tropics; a more recent developmental data set could take full advantage of a larger grid domain extending further into the tropics.

Another possible approach to improvement was to abandon the use of geopotential heights entirely in favor of deep-layer-mean winds. A preliminary exploration of this approach is discussed by Pike (1987a).

Thus, there are two broad-scale approaches to potential improvements in the NHC83 model: (1) continue using geopotential heights as predictors, correct identifiable weaknesses and gain the advantage of using an updated developmental data set, or (2) use deep-layer-mean winds as input, based on preliminary evidence that their use results in a reduction in track forecast errors. In either of the two approaches, the basic structure of the present NHC83 model would not be changed.

1.3 PURPOSE OF STUDY

This report addresses the first of the above two proposals. The essential purpose of the report is to provide documentation for this revised NHC83 model, to be known as NHC90. Work has also been accomplished on approach (2) but is only briefly addressed in the final section.

2. MODEL DEFICIENCIES

Close monitoring of NHC83 over the past several years and recent evaluations of the error characteristics have disclosed several internal weaknesses in model structure. Some of these weaknesses can be addressed and corrected while others must be considered as inherent deficiencies in this type of model or external to NHC83 and not being correctable. Still other external deficiencies can be at least partially alleviated.

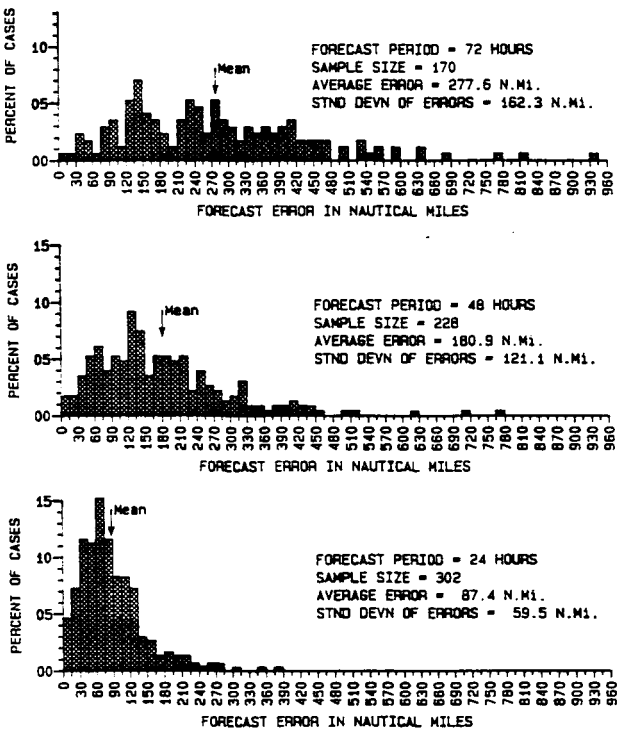

Fig. 2. Frequency distribution of NHC83 model 24, 48 and 72h forecast errors over 6-year period, 1983-1988.

2.1 NON-CORRECTABLE (EXTERNAL) DEFICIENCIES

2.1.1 Reliance on Numerical Guidance - Fig. 2 is a frequency distribution of NHC83 operational forecast errors. Comparing these errors to those of other statistical models discloses that NHC83 makes fewer "large" forecast errors. Indeed, this is one of the reasons that the overall forecast error of NHC83 is comparatively low. Since NHC83 forecasts are explicitly tied to output from the NMC Global Spectral Model (Extended 240h run, Aviation Run or Global Data Assimilation Run), this attests to the skill of the latter in projecting the large-scale steering flow and related NHC83 skill in extracting this information. There is apparently more statistical predictive information contained in these numerical prognoses than previously thought available.

Nevertheless, as shown in Fig. 2, occasional large errors, defined here as the mean plus 2 standard deviations, do occur. An analysis of the larger errors shows that they are typically caused by poor prognoses of the large-scale steering patterns. The largest 72 h error, for example (933 n mi on Hurricane Josephine, initial UTC 84101512), occurred when the Global Spectral Model mispositioned a large cold-low over the North Atlantic. In that NHC83 is explicitly tied to this numerical output, there is no practical way to avoid these occasional poor forecasts.

Since the NHC83 model was developed in the "Perfect-Prog"[4] mode, this provides a convenient method for separating the effect of errors in

[4] "Perfect-Prog: refers to the use of observed, rather than forecast fields in the model development phase.

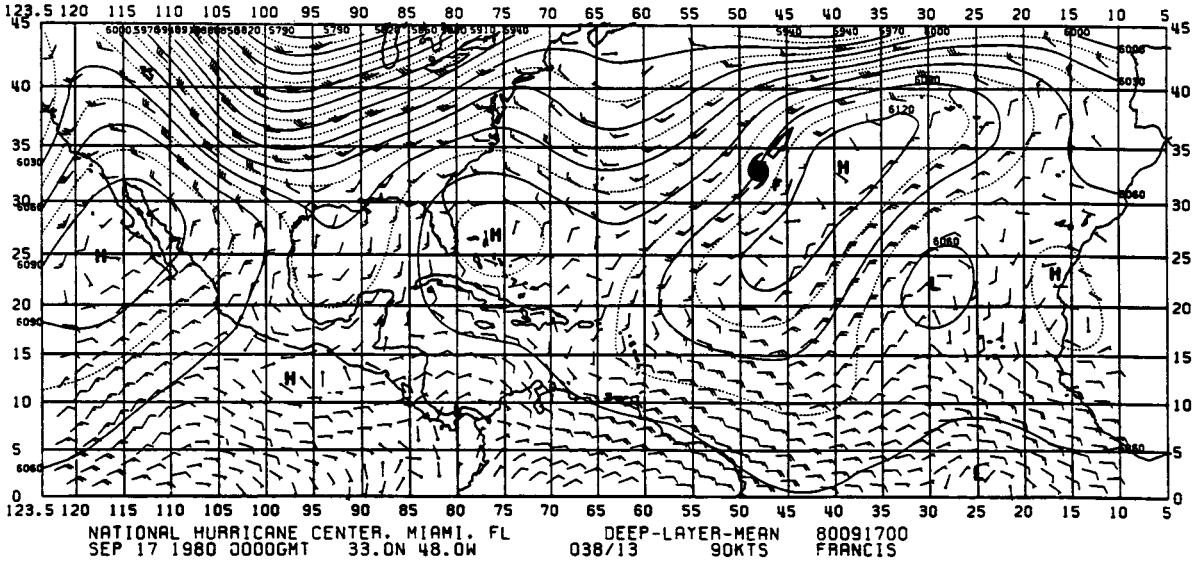

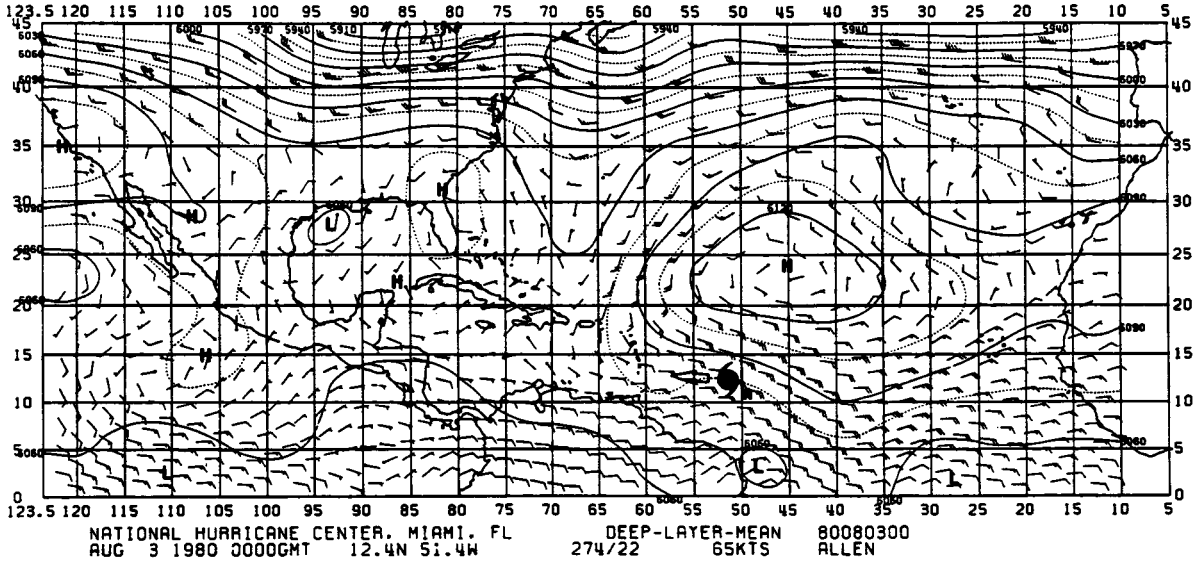

Fig. 3a. (top) and 3b. (bottom) showing examples of initial deep-layer-mean wind and geopotential height analyses where tropical cyclone vortex is not present. Upper chart is for a case after storm recurvature into the westerlies, while lower chart is before recurvature. Center of tropical cyclone (obtained from best-track of storm) is identified by darkened hurricane symbol. Heights are in meters; standard height of deep-layer-mean field is 6060.5 meters. Winds, in knots, are plotted at standard NMC grid points. Information below chart includes storm position, instantaneous motion (degs/knots) and maximum surface wind (knots) within storm at current time.

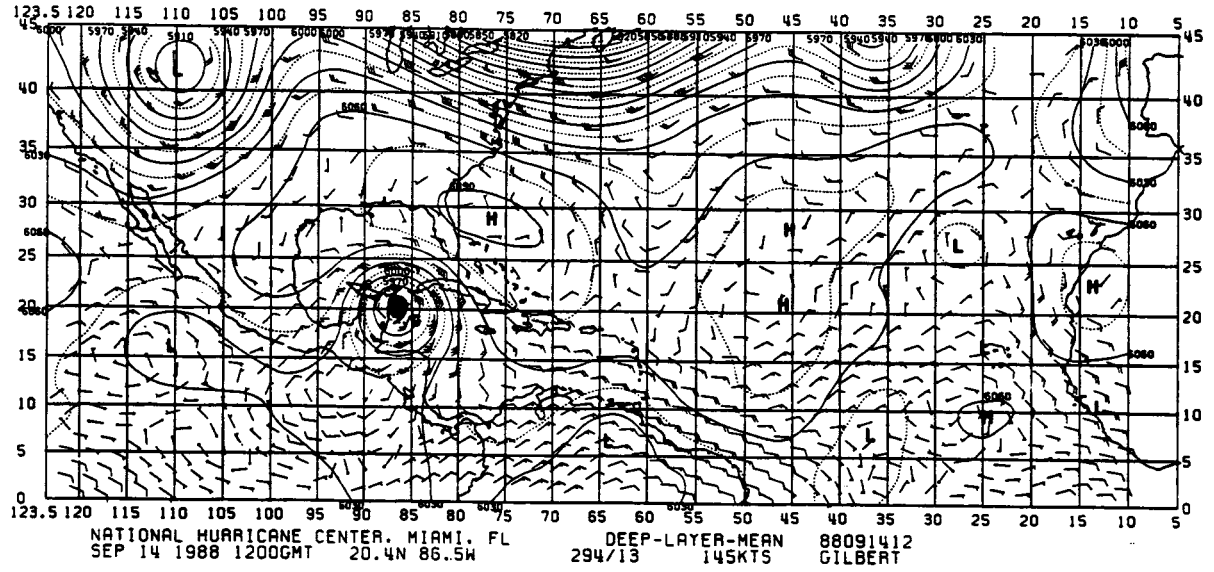

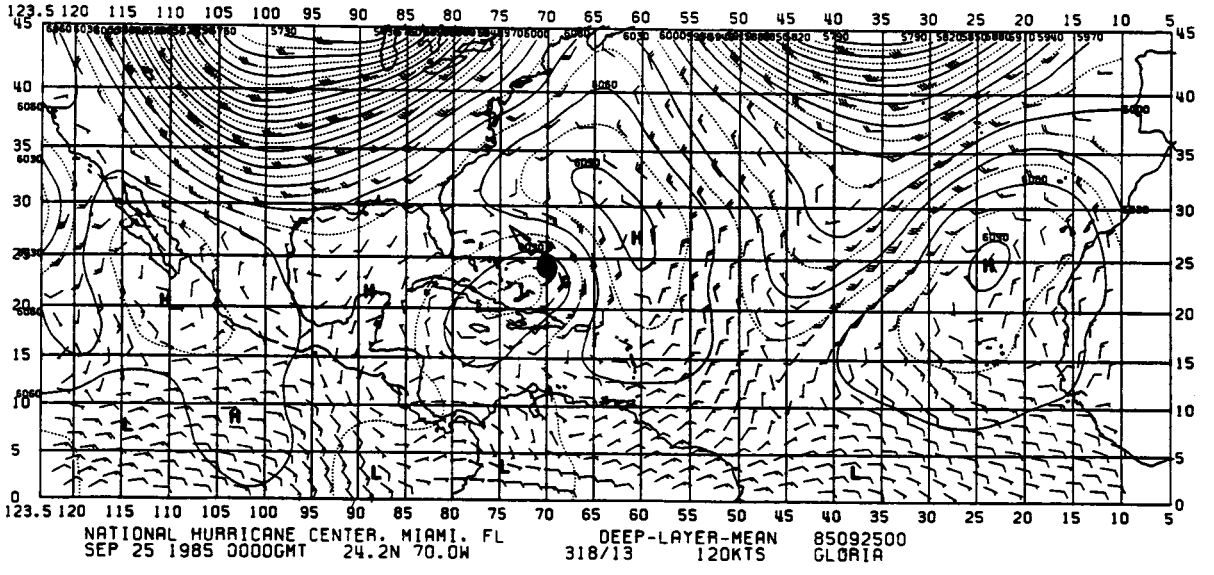

Fig. 4a. (top) and 4b. (bottom) showing examples of deep-layer-mean wind and height analyses where tropical cyclone vortex is present. Upper chart shows a reasonably correct analysis in storm vicinity while lower chart shows incorrect analysis. Other features are similar to Fig. 3.

The character of the initial analysis (and prognoses), examples of which were depicted in Fig. 3 or Fig. 4 have a profound effect on the performance of the NHC83 model. When the tropical cyclone vortex is not present, as in Fig. 3, the wind and height fields near the storm typically give an excellent indication of the steering pattern. The NHC83 model, being statistically tuned to this type analysis and prognoses gives a forecast consistent with the synoptic pattern. On the other hand, situations as depicted in Fig. 4b, depending on the location of predictors, will mislead NHC83 and result in a degraded forecast. These conclusions are based on a review of all initial tropical cyclone analyses and resulting NHC83 errors from both developmental and operational data over the period 1975-1988.

Until such time as the analysis and prognoses around the storm area becomes reasonably consistent, there is no short-term general statistical solution to the mis-analysis problem. However, to mitigate the problem, more recent data could be used to develop the model. Also, a limit could be imposed such that predictors were selected no closer than, say, 300 n mi (2 NHC83 or NHC90 grid points) from the storm center, to avoid interference from the vortex.

One possible long-term solution to the problem would be to develop a filter for removing the tropical cyclone vortex from the analyses and prognoses. Although such methodology is conceptually appealing, there are many problems. These are currently being addressed at NHC and elsewhere; preliminary findings have not been used in developing NHC90.

2.2.2 Bias in numerical forecasts - The Perfect-Prog method (see footnote 3) used in developing NHC83 assumes that developmental and operational data have similar statistical characteristics. For the years 1983 through 1986, this assumption was valid. However, for the 1987 hurricane season, the 18-layer MRF (Medium Range Forecast) model replaced the older spectral model in the operational "Aviation-Run" slot. The MRF has a cold bias which leads to an erosion of the geopotential heights (and an associated bias in the wind field) with time. This bias has been discussed by a number of authors including Saha and Alpert (1988), Epstein (1988), Schemm and Livesey (1988) and White (1988).

The bias pattern across the Atlantic for the 1987 hurricane season was shown in TM41, Fig. 21. At the 72 h projection, height biases (heights forecast too low) of over 40 meters were noted through the sub-tropical ridge line. Inasmuch as the standard deviation of the heights in that area is close to 20 meters, the heights are in error by as much as two standard deviations. This is a potentially serious forecast problem when storms are located in this area.

A bias correction methodology was introduced in NHC83 for the 1988 hurricane season (TM41, Section 5.4). However, since that time, NMC has made additional changes to the analysis/prognoses package which appear to have altered the previous bias pattern of the MRF model and interfered with the correction methodology currently in place in the NHC83 model.

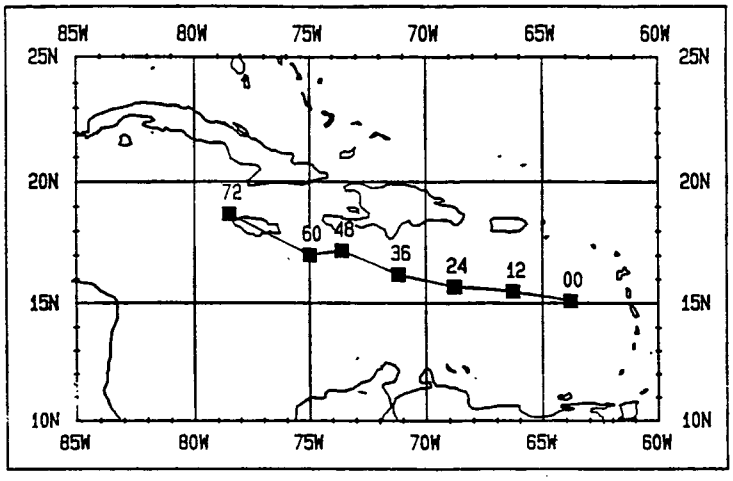

Fig.5. Example of NHC83 inconsistent track forecast at 48 and 60h for Hurricane Gilbert, Sept. 10, 1200UTC, 1988.

Until the bias in the MRF model is removed or stabilizes, there is no completely satisfactory way of compensating for it. However, in this revision to the NHC83 model, particular care was used to select predictors in pairs rather than as separate entities. Pairs of predictors allow the model to sense gradients rather than rely solely on absolute values as was sometimes done in the NHC83 model. However, this use of gradients may lead to a trade-off in predictive skill in some cases.

2.3 CORRECTABLE DEFICIENCIES

The final set of deficiencies are internal to the model and are therefore largely correctable either by re-working the dependent data or changing the set of predictors.

2.3.1 Inconsistencies in NHC83 Forecast Track - Figure 5 shows one of the operational NHC83 track forecasts on Hurricane Gilbert, 1988. Here, it can be noted that the 48 h and 60 h forecast positions appear inconsistent with other segments of the track. This inconsistency has been noted on virtually all NHC83 forecasts on storms embedded in the easterlies.

The problem here can be traced to an inconsistent selection of predictors for the 48 and 60h projections. The location of these predictors are shown in Fig. 13 of TM41 under "across-track motion, perfect-prog mode, south-zone". The predictor located some 300 n mi to the south-southwest at 48 h and at 60 h was excluded for the other forecast periods. This exclusion leads directly to the track inconsistency noted in Fig. 5. In NHC90, a consistent set of predictors was maintained for each forecast period and this deficiency appears to have been corrected.

2.3.2 Inconsistencies in NHC83 Stratification Scheme - The NHC83 model is stratified according to whether a storm is initially located equatorward or poleward from 25°N. A different prediction methodology is used in each of these two zones. The scheme assumes that a storm located in the south zone is moving with a component towards the west. Occasionally, this is not the case and relatively poor forecasts result. A partial solution to this problem had been incorporated into the NHC83 model for the 1988 season (see TM41, Section 4.5).

To permanently correct this deficiency, the NHC90 model uses a stratification scheme based on both initial latitude and direction of storm motion. Equatorward from 15°N, storms are assigned to a "South-Zone" while poleward from 25°N, storms are assigned to a "North-Zone". Between these two latitudes, assignment to a given zone is dependent on the storm initial motion. Specifics are given in Section 3.2.2.

2.3.3 Geographical Limitations in Development Data - National Meteorological Center Northern Hemisphere operational ("3 + 45") geopotential height analyses over the years 1962 and 1981 were used for the development of the NHC83 model. Prior to 1975, these data were represented on the standard "octagonal" grid system of that era which, depending on longitude, did not contain data equatorward from 10 to 13°N. Although data from the later years through 1981 did extend to the equator, the sample size was too small for developing the NHC83 model.

The NHC83 prediction scheme is such that a component of forecast motion is obtained both "along" and "across" the track of the storm.[5] Typically, the former is based on predictors to the left and right of the track while the latter is based on predictors ahead and behind the track (TM41, Fig. 14). For South-Zone storms, predictors to the left-of-track typically fell off the octagonal grid. Accordingly, for this zone, the NHC83 model relied heavily on the absolute value of predictors on the poleward side of the storm. This has aggravated problems with the negative geopotential height bias in the MRF model as discussed earlier in section 2.2.2.

Another problem with the NHC83 developmental data set was that one or more of the 10 levels needed to develop a deep-layer-mean were sometimes missing. This required computation of a deep-layer-mean with fewer than 10 levels.[6] No such geographical restriction or missing data existed for the NHC90 model. Presumably, this should lead to improved prediction, particularly for the South-Zone.

2.3.4 Predictor Selection Logic - Selection of predictors for the NHC83 model was based largely on rather strict significance criteria established by Neumann et al. (1977); however, other, mostly subjective, factors sometimes led to a relaxation of those criteria. This resulted in several NHC83 predictors as close as 150 n mi (one grid interval) from the storm center and the retention of up to four height predictors for a given forecast period.

In the NHC90 model, the same strict statistical significance criteria were used. However, subjective departures from these criteria were more limited than in the NHC83 model. This led to predictors being no closer than 300 n mi (two grid-intervals) from the storm center and the retention of no more than three predictors for a given forecast period and component of motion.

---

[5] In the NHC83 and NHC90 models, the terms "along-" and "across-track" refer to the persistence track of the storm as defined by the motion between the initial position and the position 12 h earlier.

[6] If less than eight levels were available, the case was not used.

Although this "tightening" of standards is expected to improve upon the performance of the model, this cannot be verified until the revised model has been used operationally for at least one hurricane season.

2.3.5 Graphical Output - Both models provide for a graphical display of the track forecast and numerical deep-layer-mean fields for the initital field and each of the six 12 h projections, 12 through 72 h. In the original model (NHC83) it was difficult to determine which portion of the height fields might be affecting a forecast position. Accordingly, the output for the NHC90 model additionally includes the location of predictors used for that portion of the overall forecast.

2.4 SUMMARY OF DIFFERENCES BETWEEN NHC83 AND NHC90

Differences between NHC83 and NHC90 as discussed in this Section are summarized in Table 2.

Table 2. Major differences between the original NHC83 and the revised NHC90 models. Abridged terminology is clarified in text.

FEATURE	NHC83	NHC90
Developmental Data	1962 - 1981 (excludes extra-tropical)	1975 - 1988 (includes extra-tropical)
NMC Grid type	"Octagonal"	Full Northern Hemisphere 65 x 65 grid
Stratification Scheme	Based on latitude only	Based on latitude and initial storm motion
"Pairing" of predictors	Not "paired" in deep tropics	Always in "pairs"
Predictor logic	Occasional inconsistency from one forecast interval to the next	Always consistent
Number of height predictors	Four or less	Three or less
Minimum distance of predictors from storm	150 n mi	300 n mi
Graphical Output	Does not include location of predictors	Does include location of predictors

3. DEVELOPMENT OF THE NHC90 MODEL

3.1 INTRODUCTION

In this section, development of the NHC90 model will be described. As previously pointed out, the basic structure of the new model is identical to the old. Therefore, much of the background material and details of model structure as given in TM41 will not be repeated here; the presentation will focus on differences between the two models.

Section 4.1.2 of TM41 describes the 5 sub-systems of the NHC83 model. NHC90 maintains this same structure as shown schematically in Fig. 6. Models 1, 2 and 3 are completely separate entities and each produces a forecast through 72h. Model 4 combines Models 1 and 2 while Model 5 (the final NHC90 forecast) combines Models 1, 2 and 3. As with the NHC83 model, the output from all five models can be made available to the forecaster.

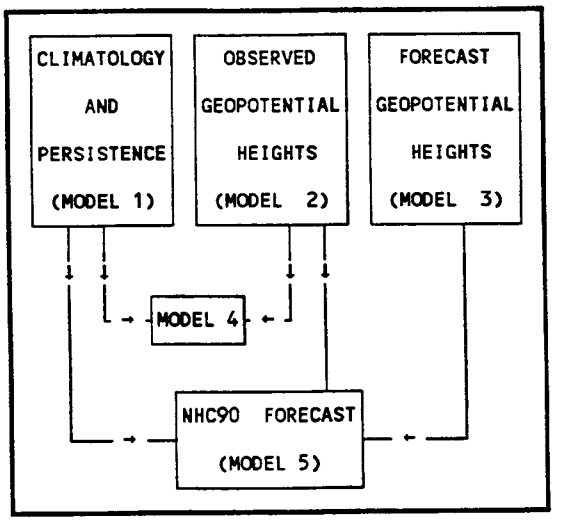

Fig 6. Schematic of the five components (models) used by the NHC83 and NHC90 models. The term DLM refers to Deep-Layer-Mean. Model 2 is referred to as "ANALYSIS" while Model 3 is referred to as the "PERFECT-PROG" mode.

3.2 DEVELOPMENTAL DATA

3.2.1 Sample size - The developmental data set used by NHC90 includes all Atlantic tropical cyclone cases having winds of at least 34 knots (tropical storm intensity or greater). Over the 14-year period, 1975-1988, positions at 0000 and 1200 UTC were used. These were paired with associated Northern hemisphere National Meteorological Center operational gridded analyses through the 72h projection. In accordance with Perfect-Prog methodology, analyses were substituted for prognoses in this developmental mode.

Although archived analyses were available prior to 1975, those analyses did not contain data in the deep tropics and use of these early data led to some problems with the NHC83 model (see Section 2.3.3). Accordingly, pre-1975 data were not used for NHC90. The total sample size available for NHC90 development was 935 cases. This is somewhat less than the 1028 cases used in developing NHC83 but is still large enough to allow stratifying the data set into two zones, a North-Zone and a South-Zone, as was accomplished with the NHC83 model.

In both models, storms which were below tropical storm strength, either at the initial or verifying position, were excluded. However, in the NHC90 model, tropical cyclones classified as extra-tropical were retained whereas in NHC83 they had been excluded. There were two reasons for this difference: (1) exclusion of the extratropical cases in NHC90 would have critically reduced the sample size; (2) inclusion of the extra-tropical cases increased, rather than decreased the variance reduction on developmental data.

3.2.2 Stratification - Stratification of a data set into two or more groups typically improves model performance in terms of real skill. However, there is also an increase in artificial skill due to the reduction in sample size. Consequently, additional stratification was avoided.

One of the most logical stratifications separates storms embedded in the easterlies (South-Zone storms) from those embedded in the westerlies (North-Zone storms). Statistically, this helps in normalizing the data set, a desirable feature in regression analysis. In Fig. 2, for example, the distribution of the 72 h errors is distinctly bimodel and this results from combining errors from storms in both zones (Crutcher et al., 1982).

There are also theoretical factors favoring a motion stratification. Storms within the easterlies tend to move to the right (poleward) from the steering flow while those within the westerlies tend toward the left (also poleward) from the basic flow (Brand et al. 1981); (Dong and Neumann, 1986); (George and Gray, 1976).

For NHC83, a rather simple criteria -- initial position poleward or equatorward from 25°N -- was used to separate storms embedded in the easterlies from those in the westerlies. As pointed out in Section 2.3.2, this was not entirely satisfactory; a somewhat more definitive system was used for NHC90:

(1) Storms initially located poleward from 25°N were assigned to a North-Zone.

(2) Storms initially located equatorward from 15°N were assigned to a South-Zone.

(3) Storms initially located between the above specified latitudes were assigned to the South-Zone only if their motion was between 180°, clockwise to 320°, inclusive. Otherwise, they were assigned to the North-Zone.

3.2.3 Statistical Attributes of Developmental Data - The statistical properties of the two data sets obtained from the above defined stratification scheme are given in Tables 3 and 4. As described in TM41, the NHC83 model prediction scheme is based on along-track and across-track components (see footnote 4). This same orthogonal system was maintained in NHC90.

The above tables are identical in format to their counterparts -- Tables 3 and 4 -- in TM41. As would be expected, there are some differences in the statistical properties of the developmental data of the two models. In can be noted, for example, that the average position of South-Zone storms in NHC90 is near 17°N whereas in NHC83, this average is near 21°N. This rather substantial difference reflects the stratification scheme between the two models. South-Zone storms being farther equatorward in NHC90 also leads to rather substantial differences in the vector motion for this zone between the two models; about 303° for NHC83 and 287° for NHC90.

For North-Zone storms, differences between the data sets of the two models are comparatively small. Indeed, most of the differences between the two models, including performance on developmental data (to be discussed in a later Section) are on South-Zone storms.

Table 3. Mean and standard deviation (n mi) of along and across track tropical cyclone displacements (predictands) for specified forecast interval in South Zone. Also given are average initial position, vector motion of storms (as defined by storm positions at -6h and +6h) and sample size.

	12h	24h	36h	48h	60h	72h
Mean along track displacement.....	136.3	265.5	387.1	496.6	593.4	664.5
Standard deviation of along track displacement.....	53.4	101.3	146.4	191.0	239.8	302.7
Mean across track displacement.....	7.5	26.3	57.3	101.1	156.4	235.4
Standard deviation of across track displacement.....	30.2	70.9	114.4	165.3	226.1	305.0
Average storm location.....	17.4N 60.5W	17.4N 60.0W	17.3N 59.3W	17.2N 58.8W	17.1N 57.8W	17.1N 57.3W
Initial vector motion..... (degs/knots)	287.1/11.2	288.0/11.3	288.6/11.5	289.0/11.6	289.2/11.7	289.9/11.8
Sample size.....	313	290	268	250	233	218

Table 4. Mean and standard deviation (n mi) of along and across track tropical cyclone displacements (predictands) for specified forecast interval in North Zone. Also given are average initial position, vector motion of storms (as defined by storm positions at -6h and +6h) and sample size.

	12h	24h	36h	48h	60h	72h
Mean along track displacement.....	138.3	263.6	352.8	416.6	469.0	515.9
Standard deviation of along track displacement.....	102.1	204.4	285.5	359.7	419.4	480.5
Mean across track displacement.....	10.9	36.1	79.9	126.6	162.7	178.7
Standard deviation of across track displacement.....	49.7	126.6	231.9	350.3	455.8	540.1
Average storm location.....	31.5N 63.6W	31.4N 62.9W	31.0N 62.6W	30.6N 62.2W	30.3N 62.3W	30.0N 62.3W
Initial vector motion..... (degs/knots)	32.4/ 8.5	31.6/ 8.1	29.0/ 7.3	27.5/ 6.8	26.5/ 6.4	26.0/ 6.1
Sample size.....	628	567	495	429	370	313

3.2.4 Composite analyses - Figures 7 and 8 present a composite analysis of storms in the North- and South-Zones, respectively. The patterns are quite similar to those shown in Figs. 15 and 16 of TM41.

The best-track average South-Zone tropical cyclone position (17.4°N, 60.5°W) is shown in Fig. 8. Significantly, the composited center of circulation is located about 100 n mi to the south-southwest of this location, near 16.0°N, 61.3°W. This is the aliasing problem discussed earlier and shown in Fig. 4b.

A closed circulation center does not appear in the North Zone composite (Fig. 7). However, the analysis suggests a vorticity center to the left of the composite best-track storm position, reflecting the frequent presence of a cold-core circulation to the west-northwest of the storm center. The analysis is unable to resolve both the cold core circulation and the tropical cyclone vortex. An example of such an analysis was depicted in Fig. 9.

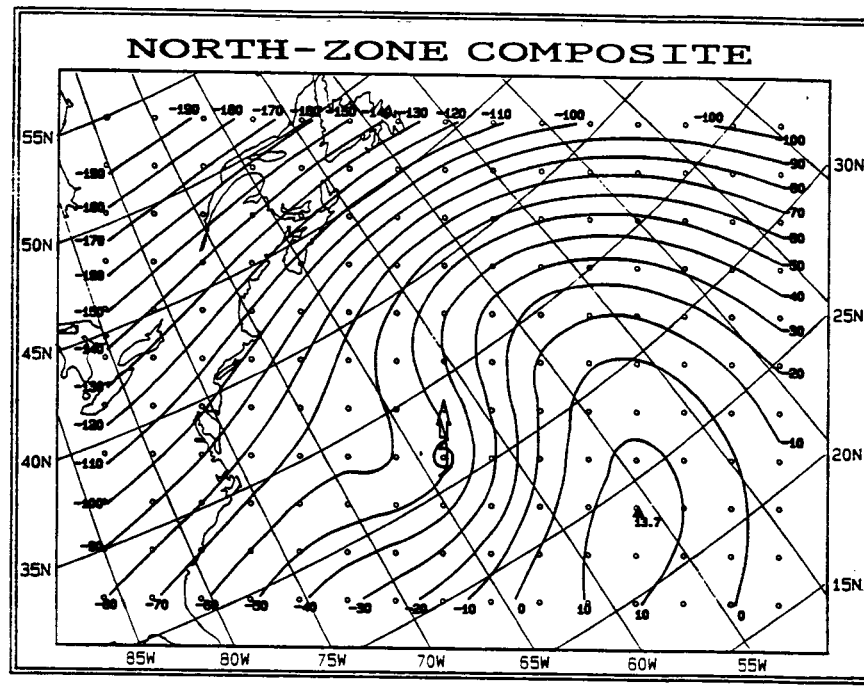

Fig. 7. Composite geopotential height field analysis for North-Zone storms. Storm is positioned at average location and is moving towards the average (vector) heading of the 628 storms used in the North-Zone as described in Table 4. Deep-Layer-Mean (DLM) contours are labeled in departure (meters) from mean September DLM height of 6060.5 meters. Darkened triangle (R) gives center of circulation as defined by maxima or minima in the field.

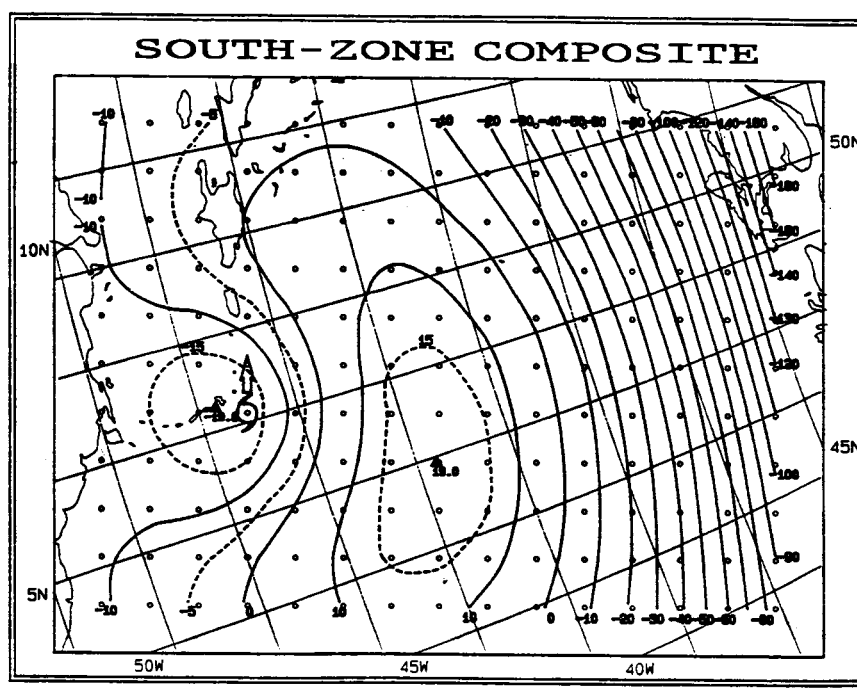

Fig. 8. Same as Fig. 4 except for 313 South-Zone cases described in Table 3.

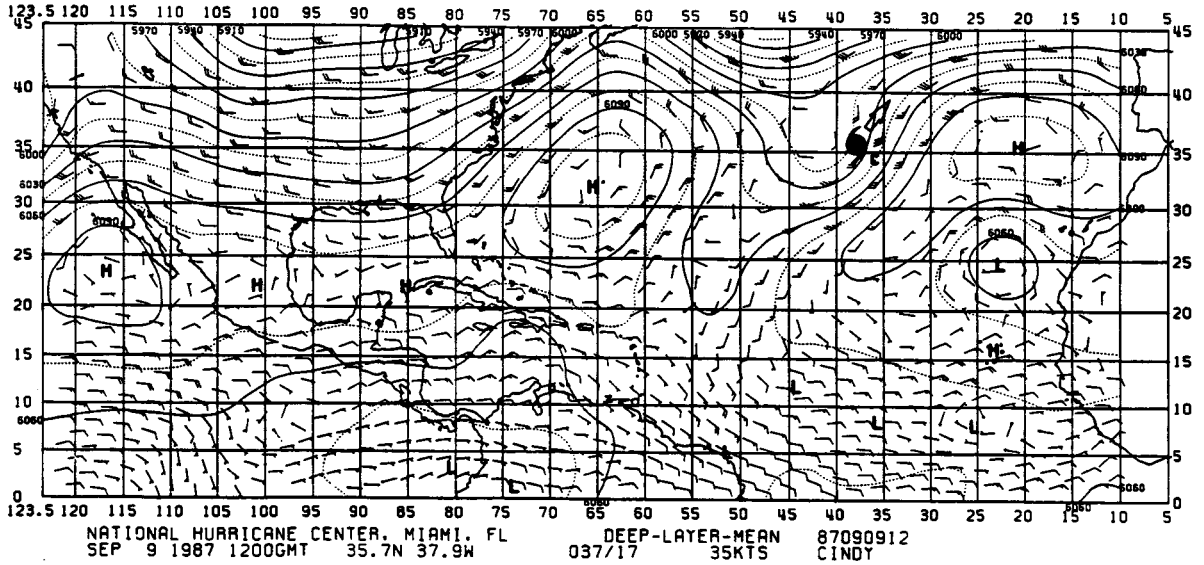

Fig. 9. Example of initial deep-layer-mean wind and geopotential height analysis showing typical cold core circulation to the west-northwest of tropical cyclone for "North-Zone" storms. Other features of analysis are similar to Fig. 3.

3.3 SELECTION OF PREDICTORS

3.3.1 Analysis mode vs. Perfect-Prog Mode - Figure 6 identified five different models which are part of the rather complex NHC83 and NHC90 prediction system. Each of these models produces a more or less independent track forecast through 72h. These tracks are then further processed into a final NHC90 forecast as described in Section 4 of TM41.

The CLIPER (Neumann, 1972) model (Model 1) does not use geopotential height predictors. However, both the "ANALYSIS" mode (Model 2) and the "PERFECT-PROG" mode (Model 3) require the selection of predictors from the NHC83 grid system (see Section 3.2 of TM41). The essential difference between Model 2 and Model 3 is that predictor selection in the former is limited to the initial analyses regardless of projection whereas in the latter, prognostic fields are used. Also, in the latter (Model 3), the height fields are averaged in time (see TM41, Section 4.3).

3.3.2 Selection Criteria - As with the NHC83 model, the selection of deep-layer-mean geopotential height predictors was based on objective and subjective considerations. Basically, the inclusion or exclusion of any given predictor was governed by objective statistical statistical significance criteria developed by Neumann et al. (1977) and Shapiro (1984) where the significance level is a function of (1) the "effective"[7] sample size, (2) the number of predictors already selected and (3) the number of remaining potential predictors. However, subjective considerations occasionally required some relaxation of these standards.

[7] The "effective" sample size refers to the number of forecast cases reduced by a factor depending upon the serial correlation between individual cases.

This relaxation was needed to force predictor selection in pairs (gradients). Pairing was considered mandatory to minimize the bias problem noted in the NHC83 model. Also, it was required to avoid the problem with NHC83 depicted in Fig. 5 where the forecast track contains unrealistic changes in motion from one forecast interval to another.

3.3.3 Pairing of Predictors - As with NHC83, selection of height predictors in the NHC90 model utilized the paired predictor concept described in Section 3.3.3 of TM41. The goal here is to insure that the two most heavily weighted predictors, which represent steering, are the best that can be selected. Considerable subjective intervention is required during this step of the predictor screening process. This is because the screening program only recognizes and selects one predictor at a time and is not sufficiently astute to recognize potential gradients. Pairs of predictors are identified by trial and error methodology where all possible pairs are tested as to their net variance reduction as well as to their consistency in the physical sense.

3.3.4 Example of Predictor Selection, North Zone, Along track - Some examples of initial predictor selection (before application of the pairing concept) are shown and discussed in this section. Examples are for the "Perfect-Prog" mode (Model 3).

Figures 10 and 11, show, respectively, the zero-order and first-order partial correlation coefficient fields (Mills, 1955) for 12 h along-track motion vs. height for the North-Zone. The counterpart of these charts, for the NHC83 model, are given as Figs. 6 and 7 of TM41 and the marked similarity between fields reflects the strong statistical stability in both models. It also reflects the fact that, except in the near-equatorial regions, the two developmental data sets (1962 - 1981 for NHC83, 1975 - 1988 for NHC90) overlap for the years 1975 - 1981.

To be noted in Fig. 11 is an area of residual negative correlation to the left of the storm after selection of the initial predictor. This reflects the fact that the selected initial grid point (column 5, row 6)[8] is not located at the exact center of correlation. Conceptually, this situation could be corrected by an adjustment of the grid system. However, it is believed that the use of predictors-in-pairs, discussed in the previous Section (3.3.3), compensates for this small loss of predictive potential.

In that the two grid-point predictors chosen from these fields (as identified on the figure legends) are actually working in harmony as a gradient but are selected as separate entities, they are not necessarily the most efficient pair (see Section 3.3.3). It can be shown, for example, that predictors located somewhat closer to the storm center (column = 6, row = 5) and (column = 10, row = 4), net a significantly greater variance reduction. This latter pair is identified by trial and error methodology, as discussed in Section 3.3.3.

---

[8] Reference point for grid (1,1) is the lower-left corner. Address of lower-right grid point is (15,1).

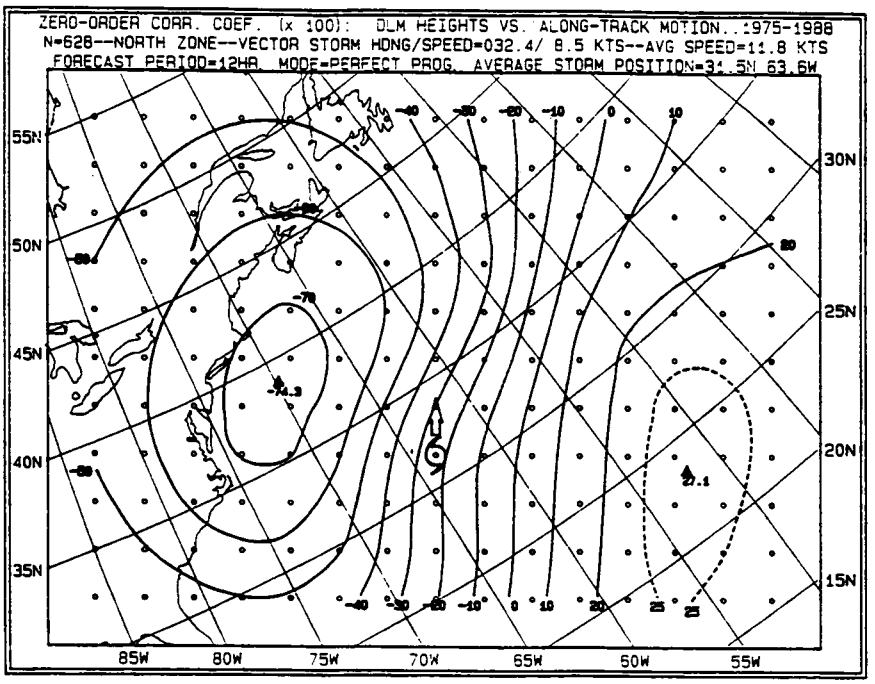

Fig. 10. Linear correlation coefficient field (zero-order partial correlation coefficient field) between 12 h along track motion and deep-layer-mean geopotential heights in the North-Zone and for the "Perfect-Prog" mode. Storm is located at the composite position of the 628 storms comprising developmental data set (see Table 4). Contours labels are in units of correlation coefficient x 100. Darkened triangles (▲) give centers of correlation. Initially selected predictor is at column 5, row 6 (reference lower left-hand corner of grid). This grid-point is located nearest to the main center of correlation.

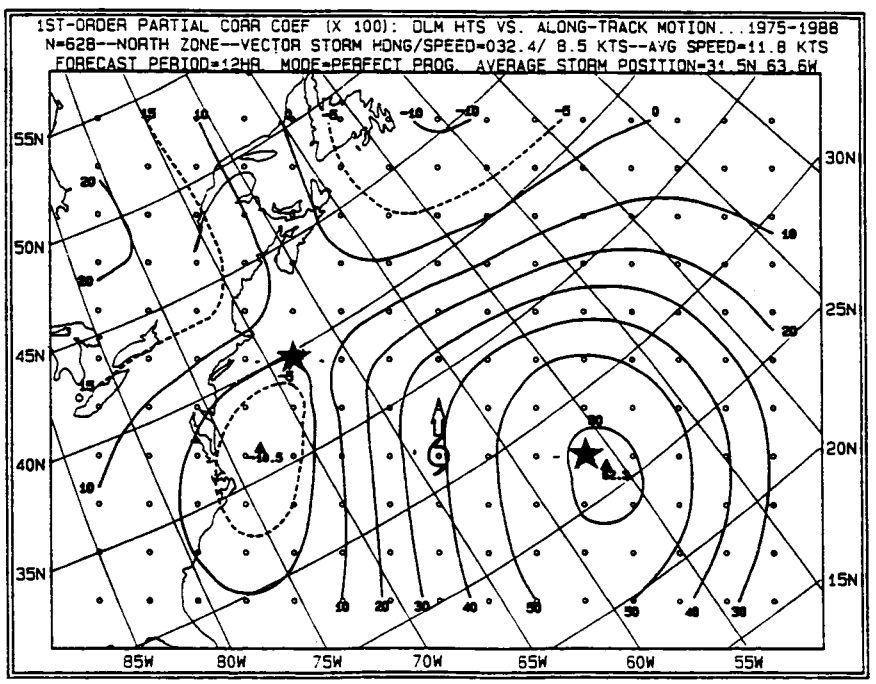

Fig. 11. Same as Fig. 10 except for first-order partial correlation coefficient field. Star (★) near 39.5°N, 68.0°W shows location of first predictor selected (see Fig. 10, above). Star near 27.2°N, 57.8°W shows location of second predictor selected. Multiple correlation coefficient associated with both predictors is 0.85.

3.3.5 Examples of Predictor Selection, North Zone, Across Track - Figures 12 and 13 are similar to Figs. 10 and 11 except that they pertain to across-track motion and are for 72 h, rather than 12 h. As discussed in TM41, Section 4.3, 72 h fields are actually average fields for the seven time periods, 00, 12, 24, 36, 48, 60 and 72 h. The averaging is accomplished after grid rotation (see footnote 5) and after translation to the observed storm position at the appropriate projection. Similarly, the 12 h fields are the average of 00 h and 12 h relative grids, etc.

Figures 12 and 13 are very similar in pattern to their counterparts, Figs. 8 and 9 in TM41. As with Figs. 10 and 11, this reflects unusual stability in the model. The two initially selected predictors, as identified in the figure legends, represent a large-scale gradient across the storm and are indicative of implied rather than direct steering. However, the predictors-in-pairs concept, discussed earlier, leads to selection of a more efficient set, positioned closer to the storm vortex and more indicative of direct steering. These latter (and final) locations of geopotential height predictors are depicted in Figs. 16 and 17.

3.3.6 Example of Predictor Selection, South Zone, Along Track - A final example of preliminary predictor selection (for the South-Zone) is given in Figs. 14 and 15. The counterpart of Fig. 14 in TM41 is Fig. 10. Because of the absence of data equatorward from the storm (see Section 2.2.3) in the NHC83 model, there is no counterpart of Fig. 15 in TM41. As was the case with the other two examples of predictor selection, the overall pattern of the correlation field is very similar between the two models.

As shown in Fig. 14, most of the predictive information for South-Zone storms is to the right, rather than to the left of the storm, as was the case for North-Zone storms. This reflects the importance of the subtropical ridge line in controlling the motion of these storms.

After the selection of an initial predictor at (column = 8, row = 5), Fig. 15 shows a weak but statistically significant area of correlation to the left-rear (southwest) of the storm. In the interest of mitigating the bias problem (see Section 2.2.2), a predictor from this area was included in the NHC90 model. This was considered an acceptable trade-off considering other risks associated with use of predictors in the deep tropics; specifically, low standard deviations of the heights used as predictors, as well as uncertainties in the analyses and numerical prognoses.

3.3.7 Final Selection of Predictors - Figures 10 through 15 showed examples of preliminary predictor selection for the Perfect-Prog mode. Similar procedures are followed for the selection of Analysis mode predictors except that the current analysis is used for every forecast interval.

After the application of predictor-pairing methodology, a further search is made through second-order partial correlation fields for areas of additional predictive information. Typically, other than for the two "steering" predictors (zero- and first-order partial

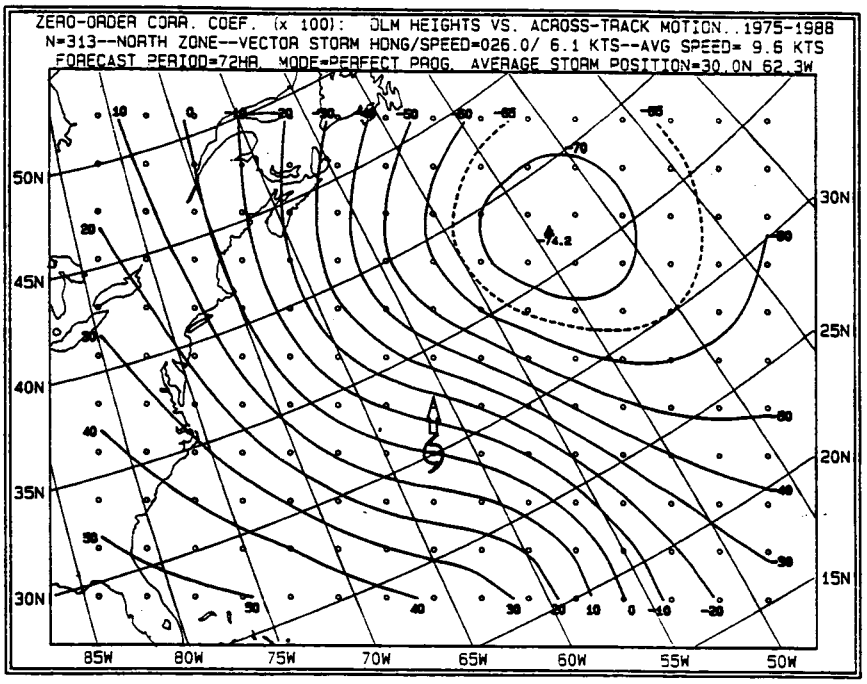

Fig. 12. Linear correlation coefficient field (zero-order partial correlation coefficient field) between 72 h across track motion and deep-layer-mean geopotential heights in the North-Zone and for the Perfect-Prog mode. Storm is located at the composite position of the 313 storms comprising developmental data set (see Table 4). Contours labels are in units of correlation coefficient x 100. Darkened triangles (▲) give center of correlation. Initially selected predictor at column 10, row 9 (reference lower left-hand corner of grid). This grid point is located nearest to the main correlation center.

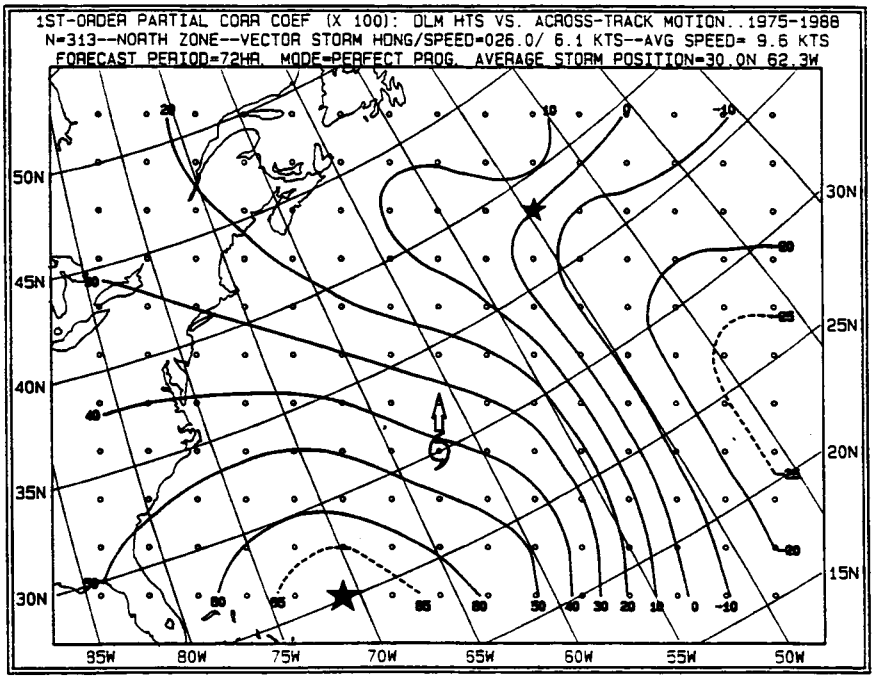

Fig. 13. Same as Fig. 12 except for first-order partial correlation field. Star (★) near 38.5°N, 49.5°W shows location of first predictor selected (see Fig. 12, above). Star near 25.1°N, 71.0°W shows location of second predictor selected. Multiple correlation coefficient associated with both predictors is 0.92.

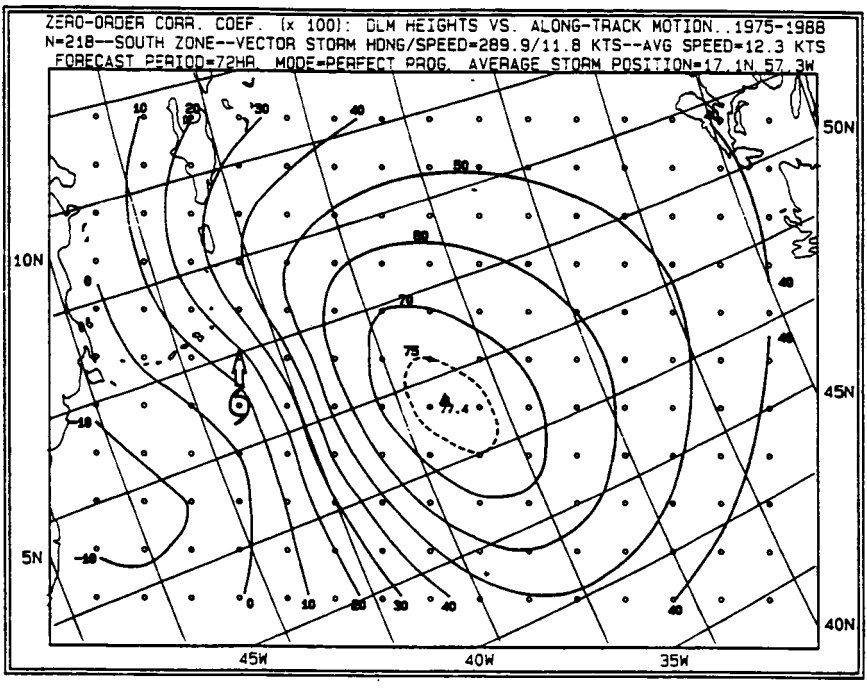

Fig. 14. Linear correlation coefficient field (zero-order partial correlation coefficient field) between 72 h along track motion and deep-layer-mean geopotential heights in the South-Zone and for the "Perfect-Prog" mode. Storm is located at the composite position of the 218 storms comprising developmental data set (see Table 3). Contours labels are in units of correlation coefficient x 100. Darkened triangles (▲) give center of correlation. Initial predictor selected is at column 8, row 5 (reference lower left-hand corner of grid).

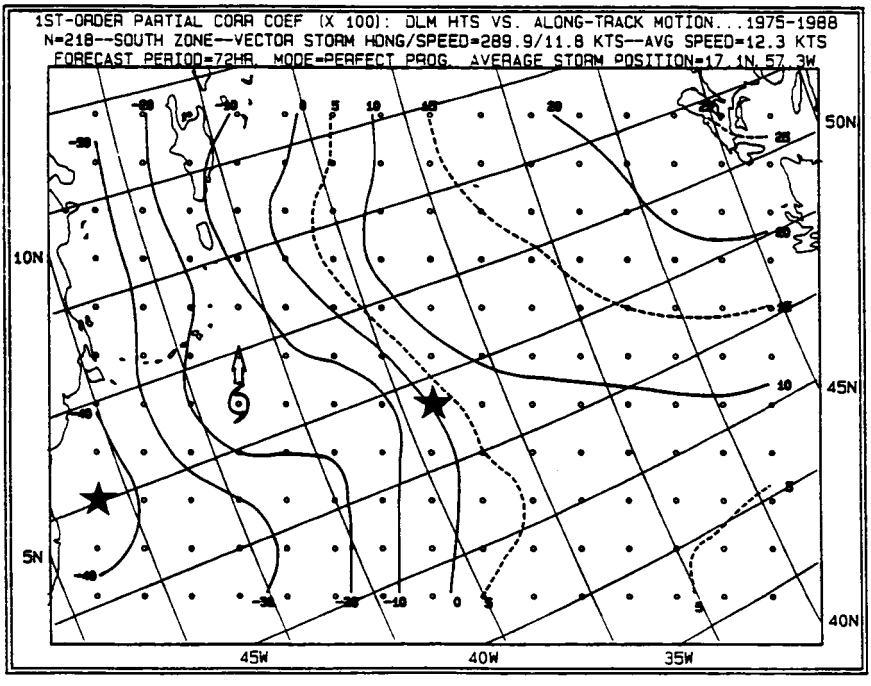

Fig. 15. Same as Fig. 14 except for first-order partial correlation field. Star (★) near 26.5°N, 53.5°W shows location of first predictor selected (see Fig. 14, above). Star near 8.0N, 55.2°W shows location of second predictor selected. Multiple correlation coefficient associated with both predictors is 0.82.

correlation fields), additional significant predictors were not found. The exception was for along-track motion in the Perfect-Prog mode where, for all projections, 12 through 72 h, an additional significant height predictor was identified to the left-of-track.

In all, there are eight sets of geopotential height predictors for each of the six projections, 12 through 72 h. Four sets are for the Analysis mode and another four sets are for the Perfect-Prog mode. Specific locations of the predictors for these modes, respectively, are shown in Figs. 16 and 17.

4. MODEL PERFORMANCE ON DEVELOPMENT DATA

4.1 REDUCTIONS OF VARIANCE

4.1.1 Review of Model Structure - As briefly pointed out in Section 3.1 and as shown schematically in Fig. 6, the NHC83 and NHC90 are developed from the output of three different models. These have been referred to as Model 1 (which utilizes only those predictors related to climatology and persistence), Model 2 (which utilizes only predictors derived from current deep-layer-mean height analysis) and Model 3 (which utilizes only predictors derived from "forecast" fields). Each of these models produces a forecast track through 72 h.

The output from these three models, in the form of along- and across-track displacements, are then used as dependent data for the development of a final forecast (Model 5). In an operational mode, Model 4 (which is a combination of Models 1 and 2) is used as a "first-guess" for positioning the grids in the numerical fields. Model 4 is not used in the developmental mode. Additional details on this process are given in TM41.

Reductions of variance which were obtained from Models 1, 2 and 3 are given in Tables 5, 6 and 7 while those from the combined Model 5 are given in Table 8. Table 5 was not included in TM41; however, the latter three tables, for the NHC83 model, appear in TM41 as Tables 5, 6 and 7.

4.1.2 Comparison of Variance Reductions - In comparing variance reductions, it should be noted that reduction of variance (R^2) is given by the relationship,

$$R^2 = 1 - S_e^2/S_y^2 \qquad (1)$$

where R is the multiple correlation coefficient, S_e is the standard error (standard deviation about the regression line, surface or hyperplane) and S_y is the standard deviation about the mean of the predictand. Thus, for given values of S_e, R^2 (and R) are directly proportional to S_y.

Because R^2 is a relative quantity, comparison of variance reductions from different models is typically obscured by differences in standard deviation of the predictands. In general, however, an examination of these tables indicates that, for the analysis mode (Model 2), the NHC83 model has somewhat higher variance reductions than does the new model. However, for the Perfect-Prog mode (Model 3), the reverse

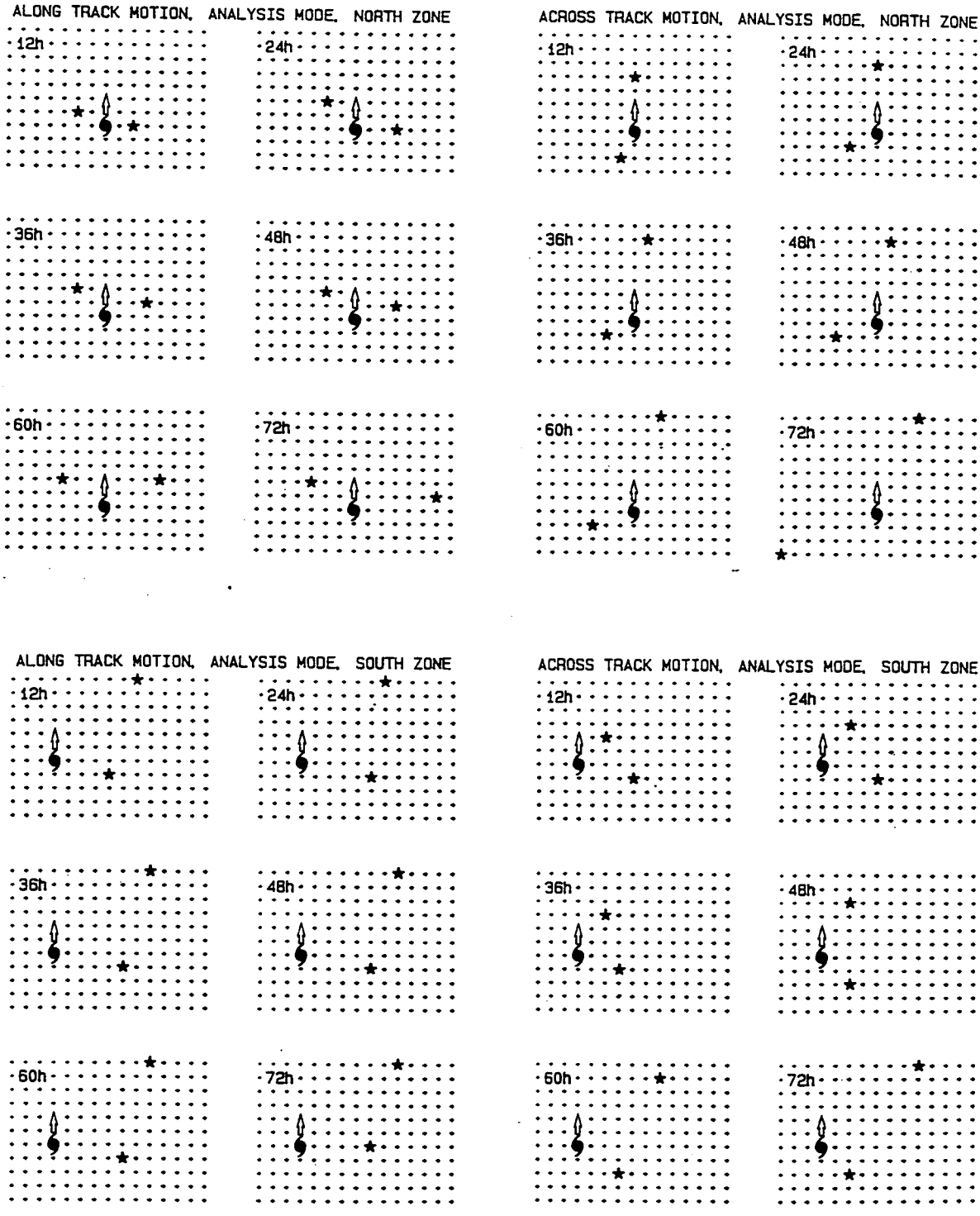

Fig. 16. Stars show location of deep-layer-mean height predictors for "Analysis-mode". Grid interval is 150 n mi (278 km). Arrow at storm location shows initial storm motion as defined by initial and 12 h old storm position. The NHC90 grid system is identical to that of the NHC83 model as described in Section 3.2 of Neumann (1988).

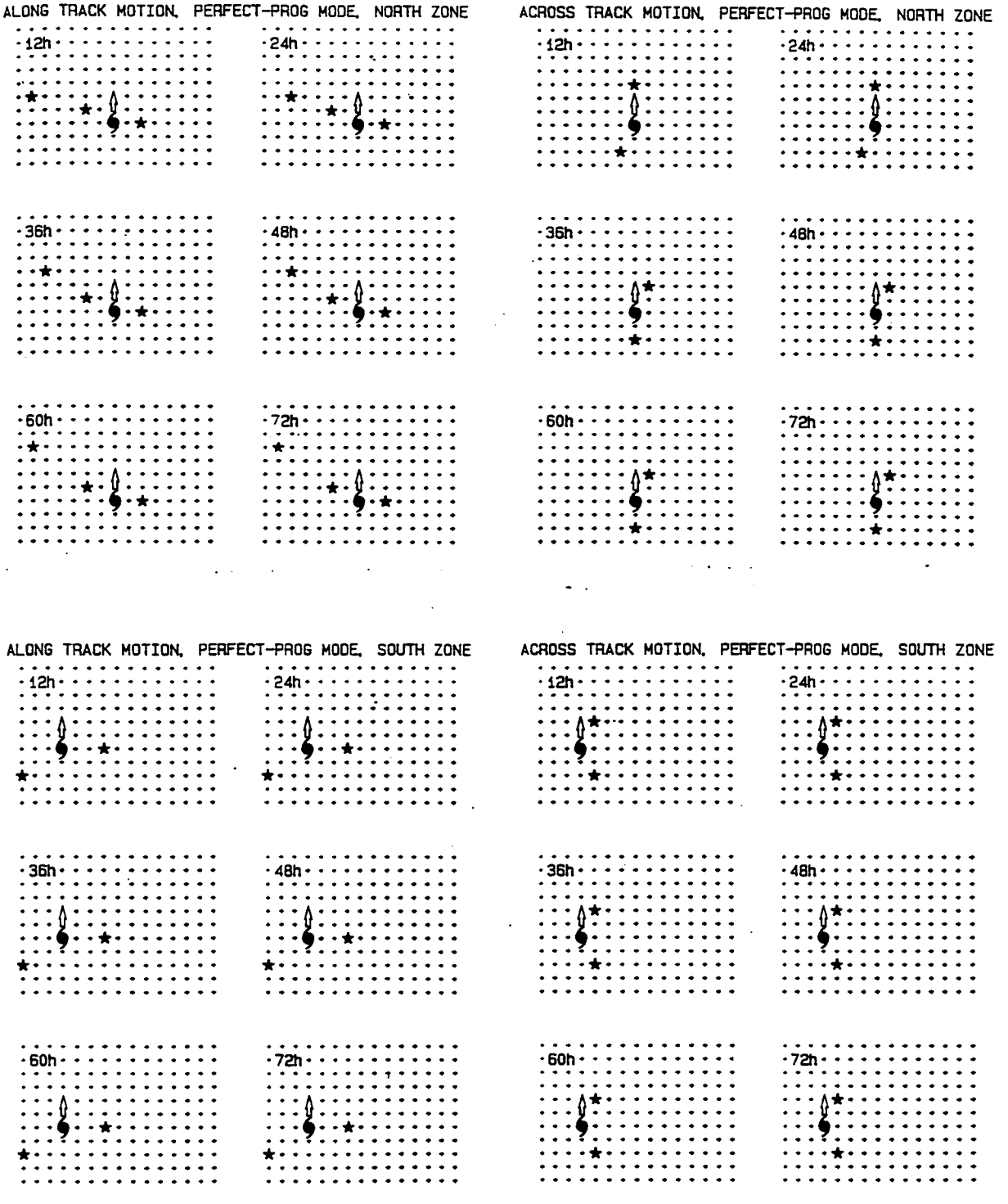

Fig. 17. Same as Fig. 16 except for "Perfect-Prog" mode.

Table 5. Developmental data [Model 1 (CLIPER mode)] reduction of variance ($0 \leq R^2 \leq 1$) of tropical cyclone motion for specified forecast interval and for specified zone and component of motion.

	12h	24h	36h	48h	60h	72h
South Zone along track variance reduction.....	0.890	0.790	0.691	0.582	0.518	0.470
South Zone across track variance reduction.....	0.734	0.540	0.440	0.393	0.400	0.386
Sample size.....	313	290	268	250	233	218
North Zone along track variance reduction.....	0.939	0.817	0.664	0.496	0.419	0.411
North Zone across track variance reduction.....	0.787	0.619	0.588	0.577	0.546	0.530
Sample size.....	628	567	495	429	370	313

Table 6. Developmental data [Model 2 (analysis mode)] reduction of variance ($0 \leq R^2 \leq 1$) of tropical cyclone motion for specified forecast interval and for specified zone and component of motion. Sample size for respective zone is same as that given in Table 5.

	12h	24h	36h	48h	60h	72h
South Zone along track variance reduction.....	0.330	0.322	0.322	0.323	0.332	0.372
South Zone across track variance reduction.....	0.118	0.170	0.232	0.243	0.258	0.315
North Zone along track variance reduction.....	0.747	0.681	0.534	0.368	0.289	0.296
North Zone across track variance reduction.....	0.347	0.401	0.456	0.451	0.397	0.362

Table 7. Developmental data [Model 3 (Perfect-Prog mode)] reduction of variance ($0 \leq R^2 \leq 1$) of tropical cyclone motion for specified forecast interval and for specified zone and component of motion. Sample size for respective zone is same as that given in Table 5.

	12h	24h	36h	48h	60h	72h
South Zone along track variance reduction.....	0.381	0.400	0.440	0.496	0.584	0.691
South Zone across track variance reduction.....	0.204	0.371	0.706	0.674	0.754	0.814
North Zone along track variance reduction.....	0.824	0.863	0.867	0.866	0.870	0.867
North Zone across track variance reduction.....	0.479	0.684	0.807	0.873	0.899	0.910

Table 8. Developmental data reduction of variance ($0 \leq R^2 \leq 1$) of tropical cyclone motion obtained by combining above three models (Models 1, 2 and 3) into a single model (Model 5...see Fig. 6). Sample size is identical to that given in Table 5.

	12h	24h	36h	48h	60h	72h
South Zone along track variance reduction.....	0.898	0.829	0.777	0.748	0.765	0.808
South Zone across track variance reduction.....	0.760	0.647	0.665	0.742	0.789	0.840
North Zone along track variance reduction.....	0.954	0.918	0.904	0.890	0.881	0.874
North Zone across track variance reduction.....	0.822	0.802	0.848	0.891	0.910	0.915

is true. The reduction of variance shown for Model 5 is greater than that for NHC83, with few exceptions. This is indeed fortunate in that Model 3 is considerably more important than is Model 2 in contributing to the skill of the final forecast (Model 5).

4.2 FORECAST ERROR

Based on developmental data, the forecast errors for the NHC90 model are given in Tables 9 and 10, for the South- and North-Zones, respectively. The error statistics for both zones combined are given in Table 11. In TM41, the counterpart of these data are given as Tables 8, 9 and 10.

A graphical depiction of the error statistics using developmental data from both the NHC83 and the NHC90 models is shown in Fig. 18. NHC90 appears to be a definite improvement over the NHC83 model for the South-Zone. Significant improvement is also seen in the North-Zone at 12 h. However, for the other North-Zone projections 24 through 72 h, there appears to be little difference between the two models insofar as developmental data error statistics are concerned.

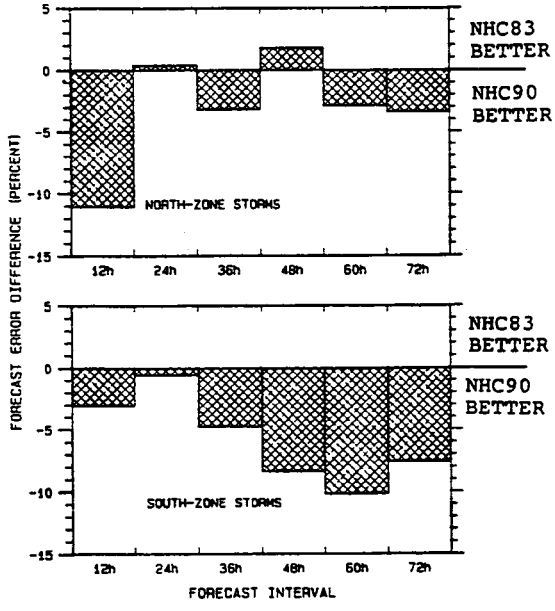

Fig. 18. Comparison of developmental data forecast errors between the NHC83 and the NHC90 models.

Considering the difference in predictor locations between NHC83 and NHC90, as discussed in Section 2, the greater improvement of NHC90 over NHC83 for South-Zone storms is not unexpected. Also, as specifically pointed out in Section 2.3.3, developmental data for the older model did not include geopotential height data for the deep tropics.

Since NHC90 performs better than the older NHC83 model on developmental data, it is to be expected that, given operational data with similar statistical attributes, this same trend will continue. However, there is never a guarantee that this will be the case. Much depends, for example, on the bias pattern of the National Meteorological Center MRF model and the character of the initial analysis in and around the storm vortex.

Table 9. Developmental (dependent data) forecast errors (n mi) on South Zone storms for Model 1 (CLIPER), Model 2 (analysis mode) and Model 3 (Perfect-Prog mode). Also given are forecast errors from Model 4 (CLIPER & Analysis) and Model 5 (CLIPER, Analysis and Perfect-Prog).

Errors from:	12h	24h	36h	48h	60h	72h
MODEL 1 (CLIPER).....	19.8	57.4	104.6	160.1	218.3	289.4
MODEL 2 (ANALYSIS).....	44.3	90.7	136.0	184.4	239.1	302.0
MODEL 3 (PERFECT-PROG).....	42.8	83.6	116.7	144.1	167.3	187.5
MODEL 4 (Models 1 and 2 combined)	19.2	54.4	98.4	148.3	197.9	255.1
MODEL 5 (Models 1, 2 and 3 combined)	18.7	50.0	82.7	111.5	137.2	158.5
Percentage improvement of Model 5 over Model 1.....	5.6	12.9	20.9	30.4	37.2	45.2
Sample size.....	313	290	268	250	233	218

Table 10. Developmental (dependent data) forecast errors (n mi) for North Zone storms for Model 1 (CLIPER), Model 2 (analysis mode) and Model 3 (Perfect-Prog mode). Also given are forecast errors from Model 4 (CLIPER & Analysis) and Model 5 (CLIPER, Analysis and Perfect-Prog).

Errors from:	12h	24h	36h	48h	60h	72h
MODEL 1 (CLIPER).....	30.1	104.0	194.5	295.3	384.5	455.7
MODEL 2 (ANALYSIS).....	55.7	129.8	221.8	330.6	429.7	506.1
MODEL 3 (PERFECT-PROG).....	47.8	89.9	126.7	158.7	184.6	210.3
MODEL 4 (Models 1 and 2 combined)	27.6	93.4	178.1	276.9	364.6	437.4
MODEL 5 (Models 1, 2 and 3 combined)	24.8	68.7	108.9	144.7	175.1	205.5
Percentage improvement of Model 5 over Model 1.....	17.6	33.9	44.0	51.0	54.5	54.9
Sample size.....	628	567	495	429	370	313

Table 11. Developmental (dependent data) forecast errors (n mi) on North and South Zones combined for Model 1 (CLIPER), Model 2 (analysis mode) and Model 3 (Perfect-Prog mode). Also given are forecast errors from Model 4 (CLIPER & Analysis) and Model 5 (CLIPER, Analysis and Perfect-Prog).

Errors from:	12h	24h	36h	48h	60h	72h
MODEL 1 (CLIPER).....	26.7	88.2	162.9	245.5	320.3	387.4
MODEL 2 (ANALYSIS).....	51.9	116.6	191.7	276.8	356.1	422.3
MODEL 3 (PERFECT-PROG).....	46.1	87.8	123.2	153.3	177.9	200.9
MODEL 4 (Models 1 and 2 combined)	24.8	80.2	150.1	229.6	300.2	362.6
MODEL 5 (Models 1, 2 and 3 combined)	22.8	62.4	99.7	132.5	160.5	186.2
Percentage improvement of Model 5 over Model 1.....	14.6	29.3	38.8	46.0	49.9	51.9
Sample size.....	941	857	763	679	603	531

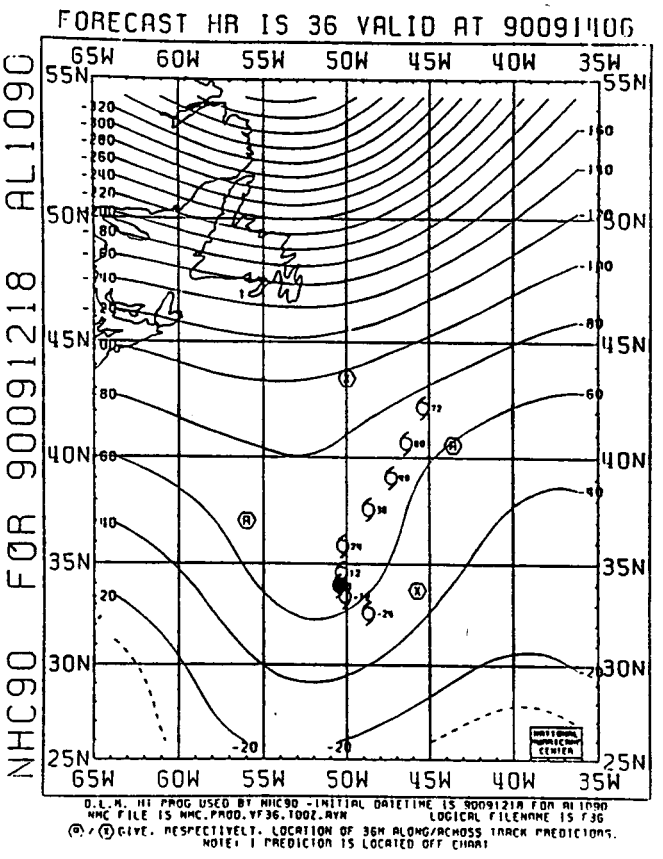

Fig. 19. Example of Chart from NHC90 graphics package. Shown are the forecast track, past storm positions and deep-layer-mean forecast geopotential height fields (departure from normal, meters) as derived from MRF model. Predictor locations are reference the Model 3 forecast which uses forecast fields and not the Model 5 track (combined final forecast) depicted.

5. GRAPHICS PACKAGE

5.1 NHC83 GRAPHICS PACKAGE

NHC83 forecasts are presented to the forecaster in both digital and graphical format. Included in the latter are the forecast track, past storm positions, the initial analysis and the six numerically forecast deep-layer-mean fields 12 through 72 h. These fields are displayed before time-averaging as discussed in Section 3.3.5. This graphics package has been particularly helpful in providing the forecaster with rationale for prognostic reasoning.

5.2 NHC90 GRAPHICS PACKAGE

For the NHC90 model, a similar graphics package was developed. However, the revised version includes the location of geopotential height predictors. Knowledge of these locations will alert the forecaster to possible problems resulting from predictors being influenced by other than broad-scale "steering-flow" fields.

Fig. 19 is an example of one of seven charts which are provided to the forecaster. Shown are the complete forecast track together with the 36 h deep-layer-mean contours from the MRF model and the location of NHC90 predictors for the 36 h projection. These predictors are shown relative to the forecast track produced by Model 3 (Perfect-Prog) and not the final forecast (Model 5) as shown on Fig. 19. Consequently, these locations may not agree with those given in Fig. 17. Predictors for the Analysis-Mode, as given in Fig. 16, being of lesser importance, are not depicted in the NHC90 graphics package.

6. POTENTIAL FOR ADDITIONAL IMPROVEMENT TO NHC90

6.1 GRID ROTATION

6.1.1 The NHC83/NHC90 System - Tropical cyclone motion is a vector quantity. Most statistical models treat both orthogonal components of motion as separate entities and then combine them to produce a vector quantity. Typically, the orthogonal coordinate system is based on earth-oriented zonal and meridional components of motion which are not independent in the statistical sense. As discussed by Shapiro and Neumann (1984), this practice leads to a slow-speed bias and increased forecast error. The authors suggested a coordinate system based on along- and across-track components where, by definition, the across-track component is initially near-zero and the forecast problem is initially univariate, rather than bivariate.

NHC83 and NHC90 are structured according to the Shapiro/Neumann system. In view of the fact that NHC83 performs very well for the short-range projections (see Section 1.2.1), the rotation system is apparently very sound. However, for the extended forecasts (beyond 36 h), there is some question as to the efficiency of the Shapiro/ Neumann system, as was pointed out by the authors.

6.1.2 Proposed NHC90 Grid Rotation System - The loss in efficiency of the Shapiro/Neumann grid rotation system for extended projections is due to gradual increases in the across-track component of storm motion throughout the 72 h forecast cycle. This is particularly noticeable for North-Zone storms where most of the storm recurvature into the westerlies takes place. As noted in Table 4, for example, the mean/standard deviation of across-track storm motion in the North Zone increases from 11/50 n mi at 12 h to 179/540 n mi at 72 h.

To compensate for this temporal loss in efficiency of the Shapiro/ Neumann grid-rotation system, Pike (1987b) suggests a grid rotation based on the axis of zero-correlation in a bivariate normal fit to the observed components of storm motion. This angle θ, (Hope and Neumann, 1970) is given by,

$$\theta = \tfrac{1}{2}\ \mathrm{TAN}^{-1}[2r_{xy}S_xS_y/(S_x^2 - S_y^2)] \qquad (2)$$

where S_x and S_y, are the standard deviations of zonal and meridional motion, respectively, and r_{xy} is the linear correlation coefficient between components. Using a period of record, 1946 through 1988, these rotation angles and related data needed by Eq. (2) are given in Table 12 for both the North- and South-Zone. Note that this period of record is (intentionally) different than that used in developing the NHC90 model (1975-1988).

Two examples of the bivariate fit to the storm motion data are shown in Figs. 20 and 21. In that the limiting chi-square value at the 0.05 probability level is 23.68 (see Crutcher et al., 1982), and in that the chi-squares computed from the data exceed this value, the bivariate fits are not particularly good. It appears that the major of the two marginal normal distributions are skewed to the right (towards higher

displacements). A bivariate log-normal distribution or a data transformation might have been appropriate here. However, this factor should not significantly affect the rotation of the major axis, which is of interest here.

The Pike rotation system is much easier to apply than is the Shapiro/ Neumann system. In the latter, grid rotation is different for each individual case. However, in the Pike system, grid rotation is fixed for a given zone and projection.

In association with the development of NHC90, a preliminary test of the Pike rotation system was conducted using the rotation angles given in Table 12. For the South-Zone, there was little difference between developmental data forecast errors for the Shapiro/Neumann system and the Pike system.

For the North-Zone, the test indicated that the current Shapiro/ Neumann system gave better results at the 12 and 24 h projections. There was little difference at the 36 h projection but the Pike system was clearly superior at 48 and 72 h. These results are similar to the findings of Pike.

This test suggests that the Pike rotation system should be incorporated into the NHC90 for the extended projections in the North-Zone and it is considered likely that this modification to NHC90 will be accomplished. The current model, however, as reported on herein, utilizes the Shapiro/Neumann system exclusively.

Table 12. Statistical properties of proposed grid-rotation system. Rotation angle (θ) is in the mathematical sense. Period of record is 1946 - 1988.

Projection		12 h	24 h	36 h	48 h	60 h	72 h
North-Zone S_x	(n mi)	109.6	200.6	278.5	347.7	411.5	467.7
North-Zone S_y	(n mi)	82.4	152.2	210.8	259.0	300.5	335.6
North-Zone θ	(degs)	25.5	26.0	26.0	25.5	25.0	24.6
North-Zone r_{xy}	($0 \le r \le 1$)	0.36	0.36	0.36	0.37	0.38	0.39
South-Zone S_x	(n mi)	56.8	109.9	164.1	222.6	289.5	354.8
South-Zone S_y	(n mi)	44.1	86.9	129.7	172.5	215.2	255.2
South-Zone θ	(degs)	-20.2	-13.4	-3.3	9.3	16.7	19.1
South-Zone r_{xy}	($0 \le r \le 1$)	-0.22	-0.12	-0.03	0.09	0.20	0.27

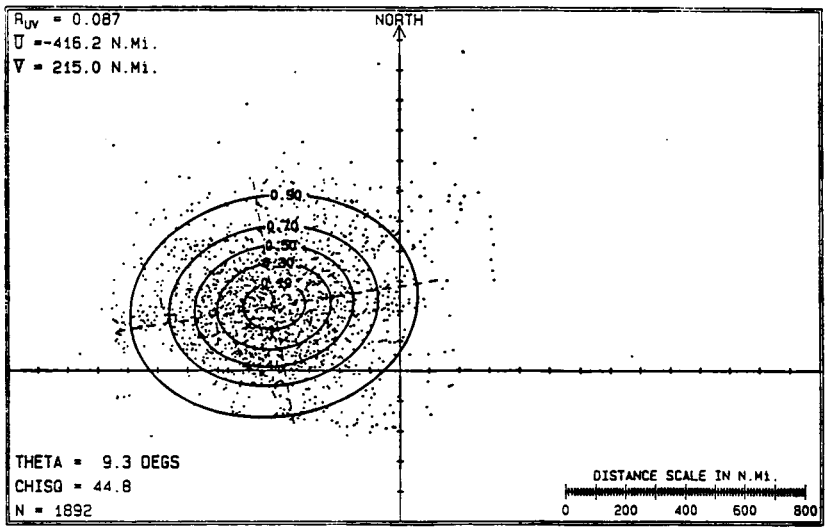

Fig. 20. Zonal and meridional components of 48 h tropical cyclone motion, 1946 - 1988, for the "South-Zone" as fitted to a bivariate normal distribution. Origin of elliptical axes indicates composited initial storm position (17.7°N, 61.4°W). Linear correlation between components, average component motion, rotation angle, value of chi-square and sample size are as specified.

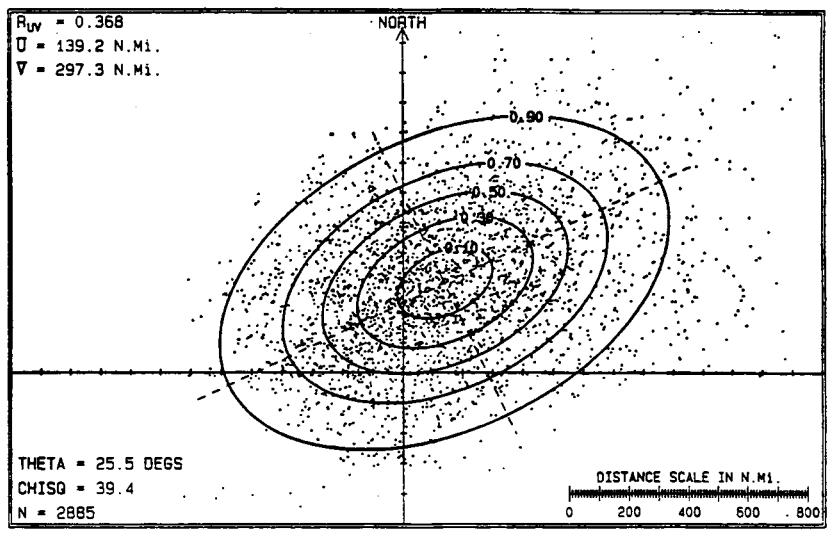

Fig. 21. Similar to Fig. 20 except for "North-Zone". Composited storm position is at 28.6N, 66.3W.

6.2 USE OF WINDS RATHER THAN HEIGHTS

Another suggested improvement to the NHC83 model involves the use of deep-layer-mean winds, rather than heights, as the main source of predictive information. A study by Pike (1987a), provided the justification and motivation for this possible improvement to the NHC83 model. Miller (1958) also studied the use of mean-layer winds as statistical predictors.

As part of the current efforts, winds have indeed been tested for their ability to improve the performance of the NHC83 model. Using exactly the same data set as described in Section 3.2, a comparison was made between the use of deep-layer-mean-winds and heights in the NHC90 model. The results are shown in Fig. 22.

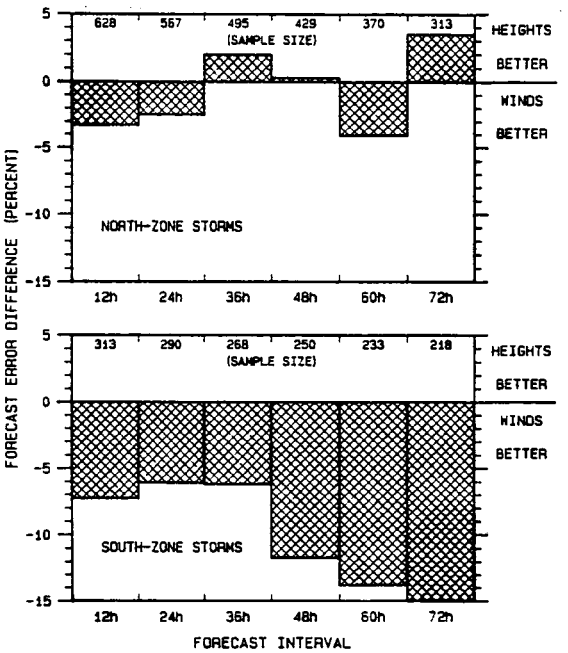

Fig. 22. 1000 to 100 mb mean heights vs. mean winds as statistical predictors of tropical cyclone motion.

Here, it can be noted that the winds, mainly in the South-Zone, provided rather substantial improvement over the heights insofar as their ability to decrease forecast error in the model. However, extending these results to operational data introduces several potential major problems which relate to initial analysis, prognoses, and the use of Perfect-Prog methodology.

A review of Figs. 10 through 15 shows that, in the case of geopotential heights, the centers of correlation and partial correlation are located at rather substantial distances from the storm center. Thus, analysis differences near the storm center, as illustrated in Figs. 3 and 4, are relatively unimportant insofar as the effect on these distant predictors. However, for deep-layer-mean winds, as yet unpublished NHC studies have shown that the centers of correlation between storm motion and along/across track wind components are very near the storm center. Accordingly, any mis-analysis near the storm center or changes in analysis methodology or numerical prognoses will have a profound effect on the value of the statistical predictor and on the final forecast from the statistical model.

This is a difficult problem to address and further discussion on the use of winds in an NHC83-type model is beyond the scope of the present study. Figure 22 indicates that winds do have the potential to improve on the performance of the NHC83 and NHC90 models. Whether these results can be extended to operational data is not known at this time.

7.0 LIST OF REFERENCES

Brand, S.C., C.A. Buenafe and H.D. Hamilton, 1981: Comparison of tropical cyclone motion and environmental steering. Mon. Wea. Rev., **109**, 908-909.

Crutcher, H.L., C.J. Neumann and J.M. Pelissier, 1982: Tropical cyclone forecast errors and the multimodal bivariate normal distribution. Journ. Appl. Meteor., **21**, 978-987.

Dong, K. and C.J. Neumann, 1986: The relationship between tropical cyclone motion and environmental geostrophic flows. Mon. Wea. Rev., **114**, 115-122.

Elsberry, R.L., W.M. Frank, G.J. Holland, J.D. Jarrell and R.L. Southern, 1987: A global view of tropical cyclones. Report of WMO International Workshop on Tropical Cyclones, Bangkok, Thailand, 1985, Office of Naval Research, 185 pp.

Epstein, E.S., 1988: How systematic are systematic errors? Preprints, 8th Conf. Numerical Weather Prediction, Amer. Meteor. Soc., 460-465.

George, J.E and W.M. Gray, 1976: Tropical cyclone motion and surrounding parameter relationships. Journ. Appl. Meteor., **15**, 1252-1264.

Hope, J.R. and C.J. Neumann, 1970: An operational technique for relating the movement of existing tropical cyclones to past tracks. Mon. Wea. Rev., **98**, 925-933.

McBride, J.L. and G.J. Holland, 1987: Tropical-cyclone forecasting: A worldwide summary of techniques and verification statistics. Bull. Amer. Met. Soc., **68**, 1230-1238.

Miller, B.I., 1958: The use of mean layer winds as a hurricane steering mechanism. NHRP Report No. 18, U.S. Department of Commerce, Washington, DC, 24 pp.

Mills, F.C., 1955: Statistical methods. Holt, Rinehart and Winston, New York, NY, 625 pp.

Neumann, C.J., 1972: An alternate to the HURRAN tropical cyclone forecasting system. NOAA Technical Memorandum NWS SR-62, National Oceanic and Atmospheric Administration, U.S. Department of Commerce, Washington, DC, 32 pp.

Neumann, C.J., 1988: The National Hurricane Center NHC83 model. NOAA Technical Memorandum NWS NHC 41, National Hurricane Center, Coral Gables, FL, 44 pp.

Neumann, C.J. and M.B. Lawrence, 1975: An operational experiment in the statistical-dynamical prediction of tropical cyclone motion. Mon. Wea. Rev., **103**, 665-673.

Neumann, C.J., M.B. Lawrence and E.L. Caso, 1977: Monte Carlo significance testing as applied to statistical tropical cyclone prediction models. Journ. Appl. Met., **16**, 1165-1174.

Neumann, C.J. and J.M. Pelissier, 1981a: Models for the prediction of tropical cyclone motion over the North Atlantic: An operational evaluation. Mon. Wea. Rev., **109**, 522-538.

Neumann, C.J. and J.M. Pelissier, 1981b: An analysis of Atlantic tropical cyclone forecast errors, 1970-1979. Mon. Wea. Rev., **109**, 1248-1266.

Pike, A.C., 1987a: A comparison of wind components and geopotential heights as statistical predictors of tropical cyclone motion. Extended Abstracts, 17th Conference on Hurricanes and Tropical Meteorology, Amer. Meteor. Soc., 101-103.

Pike, A.C., 1987b: Statistical prediction of track and intensity for Eastern North Pacific tropical cyclones. Preprints, 10th Conference on Probability and Statistics in Atmospheric Science, Amer. Meteor. Soc., J40-J41.

Saha, S. and J. Alpert, 1988: Systematic errors in NMC medium range forecasts and their correction. Preprints, 8th Conference on Numerical Weather Prediction, Amer. Meteor. Soc., 472-477.

Schemm, J.E. and R.E. Livesey, 1988: Statistical corrections to the NMC medium range 700mb height forecasts. Preprints, 8th Conference on Numerical Weather Prediction, Amer. Meteor. Soc., 478-483.

Shapiro, L.J., 1984: Sampling errors in statistical models of tropical cyclone motion: A comparison of predictor screening and EOF techniques. Mon. Wea. Rev., **112**, 1378-1388.

Shapiro, L.J. and C.J. Neumann, 1984: On the orientation of grid dystems for the statistical prediction of tropical cyclone motion. Mon. Wea. Rev., **112**, 188-199.

White, G.H., 1988: Systematic performance of NMC medium range forecasts, 1985-1988. Preprints, 8th Conference on Numerical Weather Prediction, Amer. Meteor. Soc., 466-471.